ELECTROCHEMICAL SENSORS FOR THE DETECTION OF TRICRESYL

PHOSPHATE AND DETERMINATION OF ACID CONTENT

IN ENGINE OILS

Except where reference is made to the work of others, the work described in this thesis is
my own or was done in collaboration with my advisory committee. This thesis does not
include proprietary or classified information

_____
Rigved Epur

Certificate of Approval:

_____   _____
Zhong Y. Cheng   Aleksandr L. Simonian, Chair
Associate Professor   Professor
Materials Engineering   Materials Engineering

_____   _____
Jeffrey W. Fergus   George T. Flowers
Associate Professor   Dean
Materials Engineering   Graduate School

ELECTROCHEMICAL SENSORS FOR THE DETECTION OF TRICRESYL

PHOSPHATE AND DETERMINATION OF ACID CONTENT

IN ENGINE OILS

Rigved Epur

A Thesis

Submitted to

the Graduate Faculty of

Auburn University

in Partial Fulfillment of the

Requirements for the

Degree of

Master of Science

Auburn, Alabama
August 10, 2009

ELECTROCHEMICAL SENSORS FOR THE DETECTION OF TRICRESYL

PHOSPHATE AND DETERMINATION OF ACID CONTENT

IN ENGINE OILS

Rigved Epur

_____

Signature of Author

_____

Date of graduation

VITA

Rigved Epur, son of Sri. Upender Reddy Epur and Smt. Anita Epur, was born on June 24, 1983 in Warangal, AP India. After his high school, he was selected among the top 0.8% of the 250,000 students who appeared the IIT-JEE examination, where he was selected to pursue his bachelor's degree in Metallurgical and Materials Engineering at the Indian Institute of Technology Roorkee, Roorkee, India. He also worked as a research intern at the National Physical Laboratory, New Delhi, India and Istituto Orthopedici Rizzoli, Bologina Italy where he worked on synthesizing nanomaterials for medical and optophysical applications. He then joined the Materials Engineering department at the Auburn University in 2006 under the guidance of Dr. Aleksandr Simonian where he developed electrochemical sensors for monitoring air quality in aircraft and engine oils in automobiles.

THESIS ABSTRACT

ELECTROCHEMICAL SENSORS FOR THE DETECTION OF TRICRESYL

PHOSPHATE AND DETERMINATION OF ACID CONTENT

IN ENGINE OILS

Rigved Epur

Master of Science, August 10, 2009
(B.Tech., Indian Institute of Technology Roorkee, 2006)

135 Typed Pages

Directed by Aleksandr L. Simonian

Electrochemical sensors were developed in this study for the detection of tricresyl phosphate (TCP), a toxic chemical found in airline cabins and determination of acid accumulation in engine oils upon extended usage.

A hydrolyzing column was developed that hydrolyzed TCP to electro-active cresols which were detected using a copper-nanoparticle-multi-walled carbon nanotubes modified glassy carbon electrode. The problem arised due to electrode fouling was solved using Sodium 3,5 dibromo-4-nitroso benzene sulfonate (DBNBS) reagent. An automated sensor was developed using LabVIEW$^{®}$ by integrating the hydrolyzing column, modified electrodes and potentiostat for on-site detection of TCP in airline cabins.

With extended usage, engine oil accumulates several acids by incomplete oxidation which increases the acid content of the oil. Iridium oxide coated titanium electrodes were fabricated to determine the increased acid content in artificially aged oils whose trend was in accordance with the Total Acid Number (TAN) values found by potentiometric titration. The pH sensing properties of iridium oxide were exploited for the detection of paraoxon, a toxic organophosphorus compound. An enzyme immobilized multi-channel pH sensing block was fabricated for its detection.

AKNOWLEDGEMENTS

I would like to sincerely thank my mentor, Dr. Aleksandr Simonian without whom none of this would have been possible. His continuous support, encouragement and valuable suggestions played a vital role in the achievement of this research. I would like to extend my thanks to my advisory committee members, Dr. Jeffrey Fergus and Dr. Zhong Yang Cheng for their participation in my thesis committee. I would like to thank John Curtis Addison for his help in automation of the sensor presented in the thesis. Special thanks to our collaborators Dr. David Stanbury and Dr. James R. Wild for their support and valuable suggestions during the investigation. I would also like to thank Major Leamon Viveros for his help in designing the multi-channel sensor presented in the thesis. I am grateful to my lab members Tony, Saroja, Madhu, Shankar, Sheetal, Greg, Ainur, Markhabat and Valber for their support, camaraderie and making the lab a nice place to work. I would also like to thank my friends at Auburn for making my stay cheerful and memorable.

Finally, I would like to thank my fiancée, Madhu, my parents and sister for giving emotional support and encouragement at every step while working towards my thesis.

The following peer reviewed publications and conference presentations were a product of this thesis:

Peer reviewed publications:

- Valber Pedrosa, *Rigved Epur*, Jessica Benton, Ruel A. Overfelt & Aleksandr L. Simonian, "Copper nanoparticles and carbon Nanotubes-based electrochemical sensing system for fast identification of tricresyl-phosphate in aqueous samples and air", **(2009***) Sensors and Actuators B*, **140** (1), 92-97

Conference presentations:

- Metal oxide-based pH sensor for the detection of organophosphorus compounds, 215th meeting of *The Electrochemical Society*, May 25-29, 2009, San Francisco, CA

- Electrodeposition of copper nanoparticles on carbon Nanotubes for detection of cresol by effect of electrocatalytic process, accepted for oral presentation at The 2008 *AIChE Annual Meeting*, Nov. 16-21, Philadelphia, PA

- Electrochemical detection of tricresylphosphates, 213rd meeting *of The Electrochemical Society*, May 18-22, 2008, Phoenix, AZ

Style manual or journal used:

Guide to Preparation and Submission of Theses and Dissertations

Computer software used:

Microsoft Office 2003

TABLE OF CONTENTS

xi

LIST OF TABLES

xv

LIST OF FIGURES

CHAPTER 1

INTRODUCTION

1.1 Motivation for research

The long-standing world interest in the monitoring of multiple complex parameters in environment, industry, medicine, science and technology, military and homeland security operations, etc. has encompassed broad requirements for highly reliable, sensitive and selective sensing systems. Such systems should be miniature, cost effective, long standing devices capable to discriminate between very similar compounds in highly crowded environment. Recent achievements in nanotechnology, materials science, molecular biology, etc. allow development of miniaturized sensitive systems for different applications.

There are a major concern these days owing to the growing number of incidents of flight attendants and passengers getting sick after prolonged exposure to TCP entering the cabin air due to faulty bleed air systems that is responsible for maintaining the air circulation (AFL-CIO, 2003). TCP is an organophosphorus compound that inhibits the action of acetylcholinesterase. Hence, it functions as a neurotoxin causing illnesses such as nausea, headache, axonal damage to nerve cells causing paralysis, hair loss and memory loss.

1

Due to limited medical aid available at such high altitudes, it is very important to detect this chemical during the initial stages of exposure. The monitoring of TCP will address concerns involving health and associated costs underscore the need to develop sensors that are portable, automatic and easy to use, to monitor the air-quality in flight cabins and detect TCPs in a timely fashion for the safety of people on the board. Such sensors may further help save millions of dollars annually that is otherwise lost in healthcare and work time due to sickness from TCP exposure.

Another problem concerning the field of transportation involves the quality of oil in automobiles. Advancements in land transport since the invention of motor cars or automobiles progressed from the initial 4-stroke internal combustion gasoline engine during the 1880s to fuel-efficient hybrid cars in the 2000s. With the population explosion and cross border alliances, there has also been an upsurge in the usage of these mediums to sustain the same. In the case of automobiles, the quality of engine oil, which in turn determines the life of an engine, deteriorates with use due to acid build-up, leading to poor fuel efficiency and final breakdown of the engine.

Thus, there is a critical need to develop a sensor that measures the acid content of an engine oil to enable its periodic change, which is less expensive as opposed to replacement of parts, and finally the car that may cost thousands of dollars.

1.2 Overview

The aim of this work is to develop electrochemical sensors for the determination of TCP in air and acid content in engine oils. The current chapter gives the motivation and overview of the organization of study. All the subsequent chapters are divided into two sections. The first section concerns the detection of TCP and the second section is related to the determination of acid content in engine oils. An extended application of pH sensing for the detection of paraoxon is also included in the second section. The first part of Chapter 2 gives information on TCP, its toxicity, concerns relating contamination of cabin air with TCP and the existing methods used for its detection. The second part of Chapter 2 gives a literature review on the different modes of oil degradation, the existing methods for determining the acid content and TAN in oil. This chapter concludes with the brief description on the current study that involves the development of an automated sensor for TCP detection in air and fabrication of iridium oxide based pH sensor for acid content determination in oils and its application for paraoxon detection. The first section of Chapter 3 details the objectives of the study, materials, methods used for the development of hydrolyzing media, modified glassy carbon electrodes and automation of the sensor. The second part of this chapter gives the objectives, materials and methods used for the fabrication of pH sensitive iridium oxide electrode, measurement of TAN in oils and application of the developed electrode for the detection of paraoxon. The two sections of Chapter 4 present the results and discussions of the two projects. Chapter 5 summarizes the conclusions and potential future work of this study.

CHAPTER 2

LITERATURE REVIEW

2.1 Introduction – Chemical Sensors

In living organisms, the term "sensor" can be referred to one of the sense organs namely eye, nose, skin, ear and tongue attributed to their unique ability to see, smell, feel, hear and taste respectively, to discern objects. Often, this ability was exploited to predict on the safety aspects of a particular environment for humans. For example, canaries that are known to sing all the time were used to warn the miners of an imminent danger from exposure to toxic gases such as carbon monoxide and methane, as these gases affected the birds before the miners. This practice to use canaries as living sensors gave birth to the term "canary in a coal mine" or a "climate canary" wherein a living thing is used to warn humans of an incoming danger. Nowadays, the technological advancements in science and engineering have made the use of living things to forewarn humans of a crisis, out of phase. However, man continues to get inspired and learn from these living things to create artificial systems to perform similar and only more functions.

The use of the term sensor, which is ubiquitous in the world today, often refers to the artificial system rather than a living thing, comprising of a recognition element and a transducer. The transducer converts the event of interaction between the target analyte and the recognition element into a deducible signal. Chemical sensors are a class of

sensors that are used to detect the presence of chemicals based on chemical interactions in matrix environments. Depending on the change in property such as optical, thermal, piezoelectric, magnetostrictive or electrical that is measured to transduce an event of interaction between analyte and recognition element, sensors may be classified into various categories.

2.2. Electrochemical sensors

In the case of an electrochemical sensor, an electrode is used to transduce the chemical interaction of a sensing element, which may be either on the electrode surface or in close proximity, with the target analyte into a signal that is a change in an electrical property such as voltage, current, resistance, capacitance etc. Electrochemical sensors may be classified into the following categories:

2.2.1 Potentiometric Sensors

These sensors are based on the transduction mechanism of measuring the interfacial potential at an electrode surface resulting from the chemical reaction between the analyte species and an Ion Selective Electrode (ISE) (Joseph, William et al., 2003). The voltage arising from such electrochemical reaction is measured at zero current against reference electrodes such as $Ag/AgCl$ and Hg/Hg_2Cl_2. The glass pH electrode composed of a glass membrane is the widely used ISE for the determination of hydrogen ions (pH) in solution. Several gas sensors have also been developed using ISEs over the past few years for the detection of harmful gaseous pollutants such as CO_2, CO, NO_x, SO_x, H_2, Cl_2, NH_3 etc (Chambon, Germain et al., 1999; Currie, Essalik et al., 1999; Shimizu and Yamashita, 2000). These ISEs have a membrane coated on the electrode

surface that react selectively with the target gases resulting in an interfacial potential which is measured by a potentiostat.

2.2.2 Amperometric/Voltammetric Sensors

Amperometry and voltammetry based electrochemical sensors are used for detecting species in a solution which can undergo oxidation or reduction resulting in a current that is governed by Faraday's law and the laws of mass transport (Joseph et al., 2003).

Linear Sweep Voltammetry (LSV) and Cyclic Voltammetry (CV) are the most common voltammetric techniques used to detect electro-active species present in the solution. In LSV, a potential is swept linearly with time and the corresponding current due to electron transfer to or from the analyte species to the electrode is measured **(Figure 2.1).**
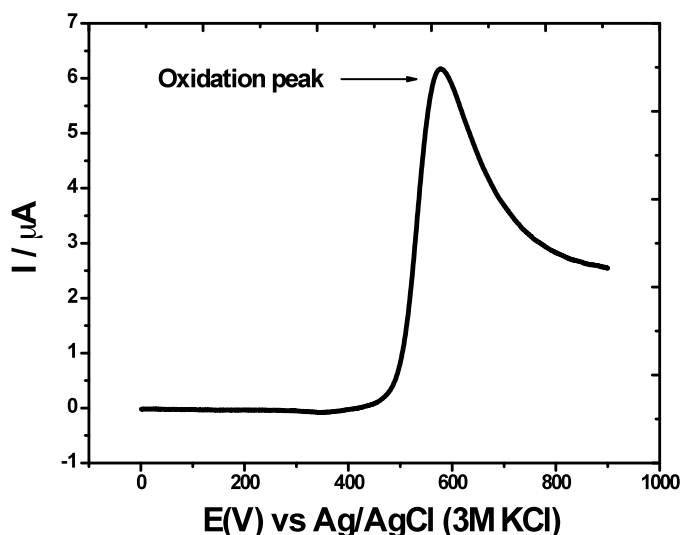
Figure 2.1: A typical Linear Sweep Voltammogram

CV is different from LSV, in that the potential at the end of forward scan is reversed to provide information on the oxidation and reduction of species that may undergo reversible reactions **(Figure 2.2).** Additional information on diffusion coefficients may also be obtained.
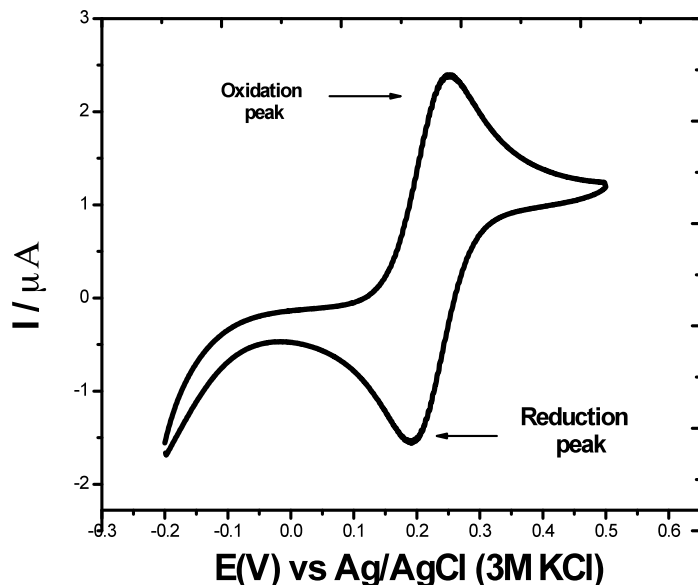
Figure 2.2: A typical Cyclic Voltammogram

In amperometric measurements, a constant or stepped potential is applied to the working electrode and the current obtained from the electron transfer due to the faradic processes is plotted against time. Amperometry is usually performed in either batch mode or in flow mode. Batch mode measurements involve the introduction of analyte to the original electrolyte solution producing a step increase in current **(Figure 2.3)**. In flow mode, the analyte is injected into the electrolyte stream which is in continuous contact with the working electrode. As the injected analyte reaches the electrode surface, it undergoes oxidation or reduction thereby giving a peak current (**Figure 2.4**).

7
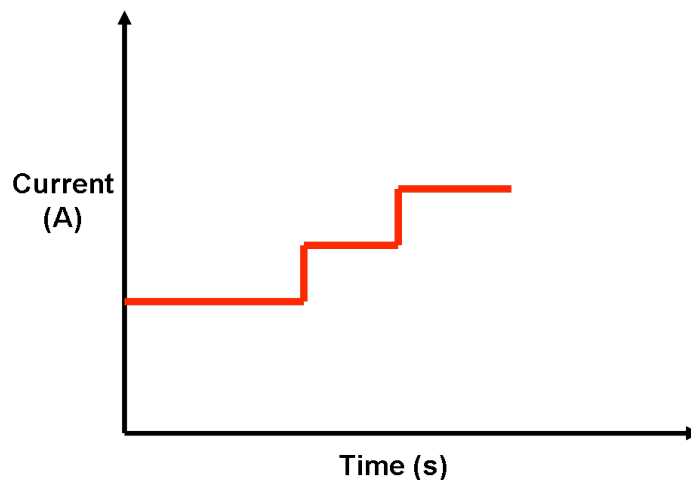
Figure 2.3: Amperometric response in batch mode
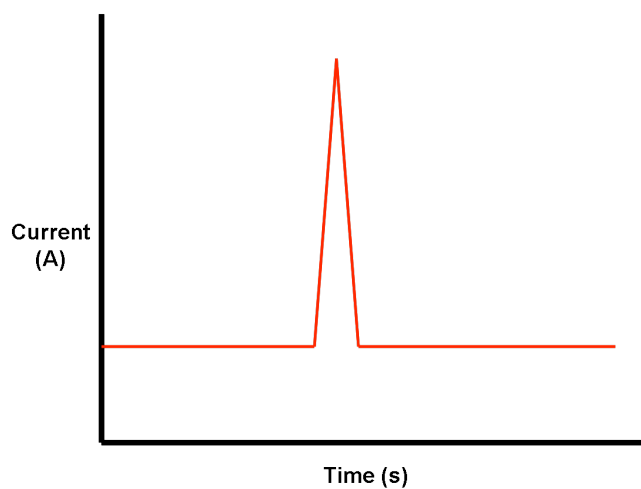
Figure 2.4: Amperometric response in flow mode

Electrochemical sensors offer advantages like high sensitivity, rapid response and minimal sample preparation. These sensors have two or three electrode cell configuration, which are connected to an amplifier, such as a potentiostat or a voltmeter to analyze the signal and translate into readable information. Recent advancements have improved the portability of the potentiostats by miniaturizing them and allowing them to

8

transfer data wirelessly to a different location thereby opening the door for remote detection of analytes.

Electrochemical sensors can be used to determine various substances present in solution or electrolyte. These sensors have diverse applications in fields ranging from medicine(Leland and Champ, 1962) to environmental monitoring (Barry, Lin et al., 2008). In addition to solution detection of analytes, there are also electrochemical sensors for detecting toxic gases such as carbon monoxide, hydrogen sulfide, chlorine, nitrogen and sulfur oxides(Chambon et al., 1999; Currie et al., 1999).

2.3 Detection of tricresyl phosphates (TCP) in air

2.3.1 Tricresyl Phosphates

Tri-cresyl Phosphate (TCPs) belongs to the class of organophosphorus compounds (OPs) which are organic tri-esters of phosphoric acid. They are high-volume production chemicals exceeding 1 million pounds in United States alone with applications in industries involved in the production of additives and plastisizers, metal working fluids and softeners (Eyer, 1995; Quintana, Rodil et al., 2008). They are often used as extreme pressure/antiware agents and as plasticizers (Eyer, 1995). They also serve as flame retardant in plastics (Reemtsma, Quintana et al., 2008), as a heat exchange media or as a lead scavenger in gasoline(Winder and Balouet, 2002; Quintana et al., 2008). For these purposes, as much as 3 % by weight of TCP is added in jet engine oils (Craig and Barth, 1999).

9

2.3.2 Chemical structure

Tri-cresyl Phosphate belongs to the class of organophosphorus compounds (OPs) which are known to inhibit the action of acetylcholinesterase responsible for neurotransmission (Chambers, 1992; Eyer, 1995; Glynn, 1999). According to the chemical structure, it is composed of a phosphate group and three cresol groups. A cresol is an organic compound, also known as methylphenol in which a methyl ($-CH_3$) group is substituted onto a benzene ring of a phenolic compound. These cresols can be either ortho, meta or para cresols, depending upon the substituted position of the methyl group with respect to the –OH group on the benzene ring. The structure of generic form of TCP molecule, the phosphate group and the different types of cresols are shown in the **Figure 2.5.**

Tri Cresyl Phosphate

Phosphate   O-cresol   p-cresol   m-cresol
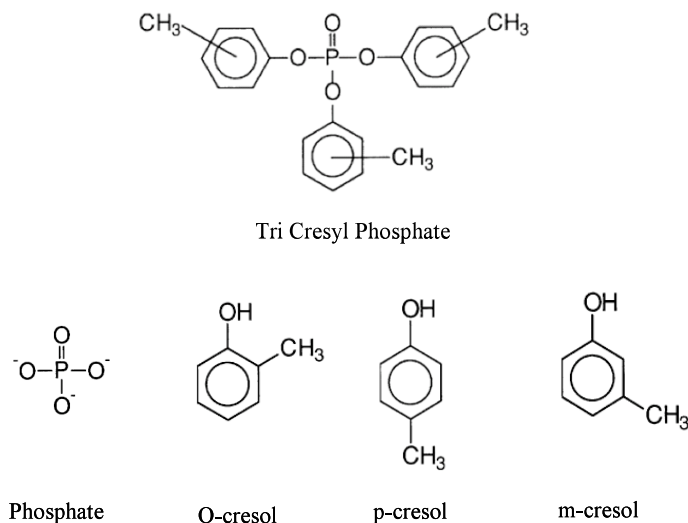
Figure 2.5: Chemical structures of Tri-cresyl phosphate, phosphate group, o-cresol, p-cresol and m-cresol

10

TCP is manufactured industrially by the oxidation of phosphorus trichloride with cresols(2007). Commercial grade TCP is a mixture of different isomers (ortho, meta and para) of TCP and is called by different names such as Tritolyl phosphate, Phosphoric acid tritolyl ester, Cresyl phosphate, Tris (methylphenyl) ester of phosphoric acid, Phosphoric acid tris (methylphenyl) ester, Phosphoric acid, Tolyl ester, Tolylphosphate, Tricresyl phosphate and Tris (tolyloxy) phosphine oxide (2007).

TCP is known to inhibit esterase enzymes such as cholinesterases (Aldridge, 1953) and neurotoxic esterases (NTE) (Johnson, 1970) by a mechanism called phosphorylation. Cholinesterase enzymes help in breaking down the choline esters such as acetyl choline, which are responsible for neurotransmission. The inhibition of these esterases by the OP compounds result in the accumulation of choline ester levels leading to cholinergic overstimulation thereby producing symptoms like headache, slurred speech, lethargy, vertigo, hypothermia in living beings from exposure (Eyer, 1995). The neurotoxic esterases are responsible for transport of nutrients and energy molecules between the cell body and nerves (axons). The phosphorylation of these esterases by OP compounds causes disruption at the end of nerves causing swelling of the axons (Abou-Donia and Lapadula, 1990). Prolonged exposure causes phosphorylation of more esterases further causing cell damage leading to Organophosphorus Induced Delayed Neuropathy (OPIDN). The symptoms during the OPIDN are proximal limb paralysis, weakening of neck muscles and inhibition of respiratory muscles.

Among the three isomers of TCP, the ortho isomer namely, Tri-ortho cresyl phosphate (TOCP) is considered to be more neurotoxic than others (1990). In addition, the toxicity of a TCP mixture is dependent on the proportion of each isomer present. Studies have shown that TOCP, apart from causing neurotoxicity, it was also found to affect other functions like reproductive capability in hens (1997).

2.3.3 TCP exposure in aircraft

The aircrafts that were manufactured in the early 20th century, were meant to fly at low altitudes of few hundred to few thousand feet. On the other hand, modern aircrafts are designed to cruise at altitudes touching 30,000 ft above the sea level to have reduced air drag (Spengler and Wilson, 2003). At such high altitudes, it is critical to maintain clean, safe and a comfortable atmosphere in the air cabins. To maintain an efficient air circulating system in the cabin, airline companies employ a method called 'bleed air system'. In the bleed air system, about 50% of the total cabin air is taken in from the engine turbine and pumped to the cabins after it passes through several filters and heat exchanging chambers (Hunt and Space)**.** The other 50% of the air is the re-circulated cabin air pumped in from the recirculation system. The return air grills present on the sidewalls of the floor on either sides of the cabin takes in the exhaust air for recirculation. This enables complete exchange of cabin air with freshly circulated air approximately every two to three minutes. This system used for maintaining a clean and safe cabin air is called Environmental Control System (ECS)(Spengler and Wilson, 2003).

Jet engine oils use different isomers of TCP as a plasticizer and as a heat exchanging medium to improve its lubricating and load bearing properties in an engine (Cottington and Ravner, 1968; Craig and Barth, 1999; Netten and Leung, 2000). These oils are usually contained in the engine but are well separated from the compressor by strong metallic seals. However, these seals tend to break at times under high temperature and pressure conditions, resulting in the oils containing TCP to be vaporized. People on board are exposed to these TCP vapors as they contaminate the bleed air systems that enter the cabin air which later on gets re-circulated (AFL-CIO, 2003). Ill health effects such as vomiting, nausea, irritation and dizziness ensues. Prolonged exposure may also lead to various neurological problems (Eyer, 1995).

TCP exposure in airline cabins affects nearly 200,000 passengers every year (Gutierrez, 2009). According to an Inspection Bulletin released by the British Aerospace in March 2001, the incidents relating to the impaired performance of the crew members were due to the continuous exposure of the oil leaking into the cabins (AFL-CIO, 2003). Also, numerous testimonies were reported by flight attendants, pilots and crew members getting sick after being exposed to the fumes of the hydraulic fluids (Hunt and Space; Murawski, 2003; Gutierrez, 2009). Steps have been taken to enforce standards on the quality of air in these aircrafts. Standard 161-2007 is such a standard set by the American Society of Heating, Refrigerating and Air-Conditioning Engineers (ASHRAE) (2007; Angel, 2008) for the air quality in commercial aircrafts that is considered safe for a flight. Major studies on cabin air quality have since been launched (Dunlop, 2007) to ensure a safe and comfortable flight. Owing to the limited medical aid available at high altitudes

in an aircraft, it very important to have a fast, continuous, sensitive and rapid detection of TCP in case of exposure.

2.3.4 Methods of detection for tricresyl phosphate

Conventional methods employed for the detection of TCPs in air, water and soil include Gas Chromatography (GC) and Thin Layer Chromatography (TLC). Colorimetric and Ultra Violet Spectrometric methods may be used to differentiate the presence of TCPs from other aryl phosphates in liquid samples. Some of the methods normally employed for the detection of TCPs are discussed below:

2.3.4.1 Chromatographic techniques

Chromatography techniques in combination with various detectors like Nitrogen Phosphorus Detector (GC/NFD) and Flame Photometric Detector (GC/FPD) are used to separate and detect as low as 2 ppm TCPs (Habboush, Farroha et al., 1995). Challenges in their detection due to the presence of Triaryl phosphates (TAPs) may arise (Ramsey, Lee et al., 1980), which can be addressed by using gas chromatography in combination with mass spectroscopy (GC/MS) (Kenmotsu, Nakagiri et al., 1983). Chromatography methods coupled with various detectors may also be used to detect the cresols that are obtained from alkaline hydrolysis of TCPs. A recent study shows the use of gas chromatography coupled with mass spectroscopy (GC/MS) to separate and detect isomers of TCPs after base cleavage (De Nola, Kibby et al., 2008). However, chromatographic techniques are expensive, bulky instruments requiring skilled personnel for their

operation. Hence, they are limited to laboratory use and are difficult for applications involving onsite detection of TCPs in an aircraft.

2.3.4.2 Spectroscopic methods

TCP in lubricating oils have been detected spectroscopically, by measuring the phosphorus content at 518 nm in a cool hydrogen-nitrogen diffusion flame (Elliott, Heathcote et al., 1972). Concentrations as low as 0.009% phosphorus content were detectable using this method. However, this method suffers from poor selectivity resulting from the presence of organic solvents as interferents during flame emission.

Although the chromatographic and spectrometric techniques are sensitive and allow for the simultaneous detection of multiple isomers of TCPs, they are usually time consuming and labor intensive. In addition, the equipment for the detection or separation analysis is bulky preventing its deployment for onsite detection purposes.

2.3.5 TCP hydrolysis

Electrochemical sensors offer the advantages of simple operation and providing on-site detection capabilities as opposed to the conventional chromatography techniques with sophisticated detectors. However, TCP not being an electroactive compound prevents its direct detection by electrochemical method. However, tricresyl phosphates are known to hydrolyze in neutral, acid and alkaline media (Belski, 1977) producing corresponding cresols, di-cresyl phopshate and phosphoric acid. Cresols are the only electro-active species among these products, thereby allowing for electrochemical detection. The kinetics of the hydrolysis depends on the type of hydrolyzing media.

Neutral and acidic hydrolysis of TCP and its structural analogue tri phenyl phosphate (TPP) is relatively slow in producing cresols. However, the hydrolysis can be accelerated by using alkaline media and boiling conditions (Collins, 1945; Haslam and Squirrell, 1952).

2.3.6 Current work

In this work, an alkaline hydrolyzing media was used for the conversion of TCP to cresols. During the alkaline hydrolysis, the hydroxide ion (OH^-) acts as a nucleophile and attacks the phosphorus atom leading to the cleavage of the phenolic compound, cresol (Wolfe, 1980). The reaction pathway is shown in the **Figure 2.5**. Following the cleavage of first cresol, another (OH^-) group attacks the phosphorus center in a similar manner, leading to the cleavage of second cresol molecule. As the reaction proceeds to completion in the presence of strong alkaline media, three molecules of electro-active cresols and a phosphoric acid is generated.
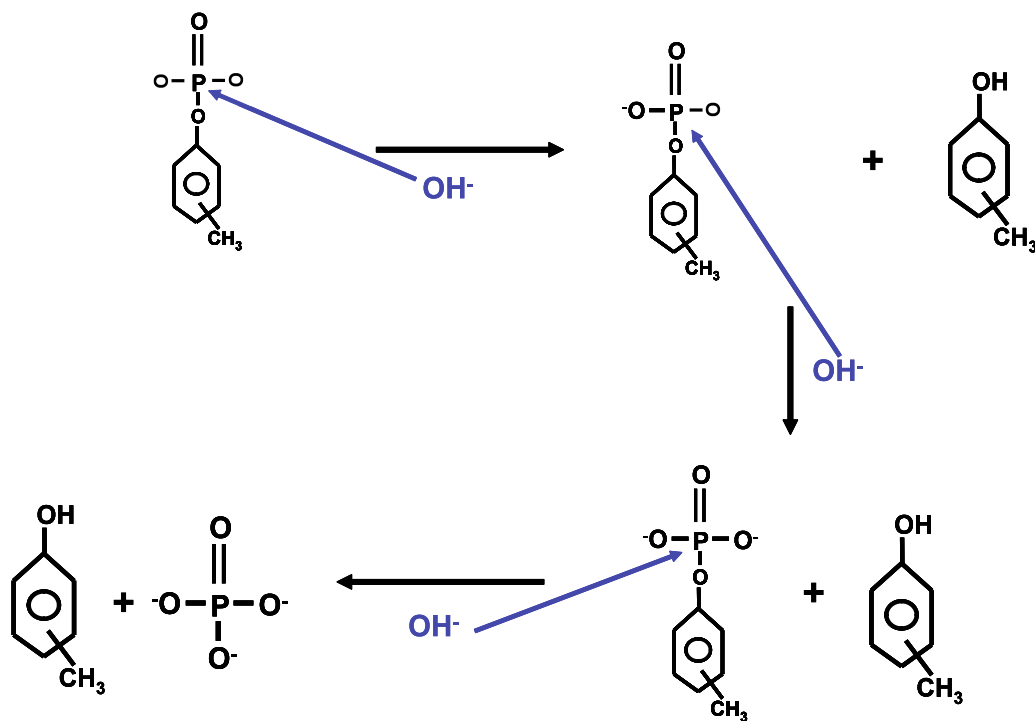
Figure 2.6: Reaction pathway for alkaline hydrolysis of TCP

In this study, an electrochemical sensor was developed to detect the cresols generated upon the alkaline hydrolysis of TCP. The cresol detection was based on its electrochemical oxidation on the surface of glassy carbon electrodes. The glassy carbon electrode was modified with multi-walled carbon nanotubes and copper nanoparticles to exploit their synergistic effect in producing catalytic current thereby enhancing the sensitivity of detection. Fouling of the electrode, which is a major concern was solved by using an anti-fouling agent namely, Sodium 3,5 dibromo-4-nitroso benzene sulfonate (DBNBS). Automation was done by using LabVIEW® to enable onsite detection of TCP in air.

2.4 Determination of acid content in engine oil

2.4.1 Motor oil

Motor oil or engine oil is a fluid that is used as a lubricant in an automobile engine. In addition to providing lubrication for the moving parts of an engine, it offers to inhibit corrosion of metal parts, cool the system by removing heat, reduce the wear and tear, and act as an anti foaming and cleansing agent. They are primarily composed of hydrocarbons, made of carbon and hydrogen atoms. Other organic and inorganic compounds are also added to the oil enhance its lubrication properties (Eilhard, 1996). These additives are consumed and depleted overtime and thus need to be replaced to provide lubrication and its other functions. Failure to replenish the degraded oil with new oil leads to problems like low mileage, corrosion of metal parts, sludge formation and increased stress on the moving parts which ultimately decrease the lifetime of the engine.

2.4.2 Stages of oil degradation

The degradation of oil in an engine can be divided into various stages depending on the number of miles covered or the extent of oil used **(Figure 2.7)**. Electrical conductivity of oil was measured over a period of time to determine these stages of degradation (Basu, Berndofer et al., 2000). In the initial stages (Stage 1 & 2), the degradation of oil was mainly due to the depletion of additives such as detergents and antioxidants. These additives serve to consume the acids produced from the incomplete oxidation of oil. In Stage-3, an increase in the acid content of the oil, otherwise known as the TAN value is observed which can be attributed to the depletion of additives from

their consumption. **Table 2.1** shows the changes in properties of oil observed in various

stages of their degradation.
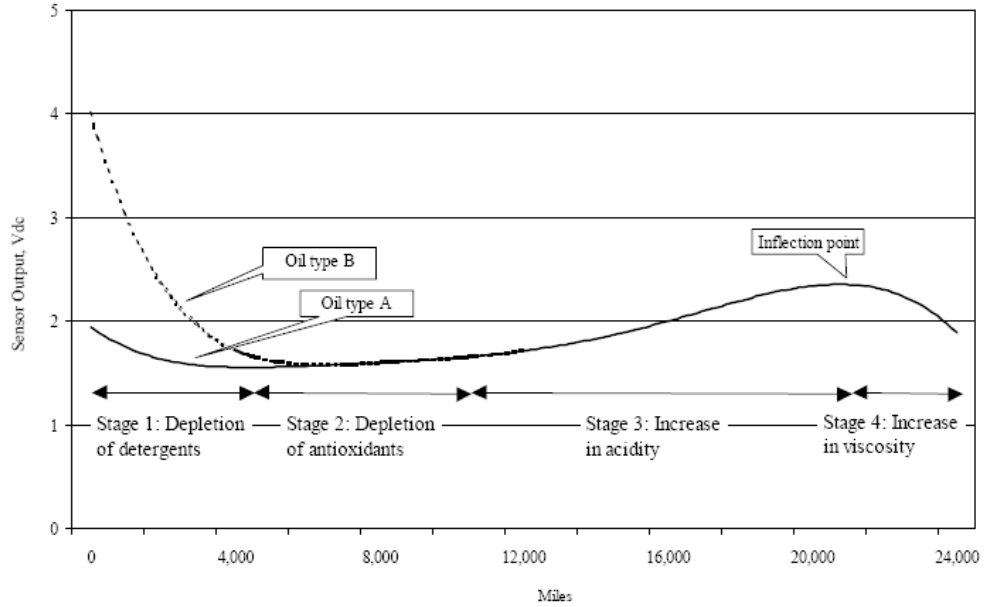
Figure 2.7: **Oil conductivity trend with mileage (Basu et al., 2000)**

Stages of degradation	Detergent, related compounds	Antioxidant, related compounds	TAN	Viscosity	Sensor output
Stage 1	Begins to inactivate	No change	No change	No change	Various
Stage 2	Complete inactivation	Begins to inactivate	Gradual increase	No change	Steady
Stage 3	-	Complete inactivation	Increase	Increase	Gradual increase
Stage 4	-	-	Continued increase	Increase	Gradual decrease

Table 2.1: Stages of degradation of oil (Basu et al., 2000)

19

The primary reason behind the change in the TAN or the acidity of the oil is due to the change in the chemical composition, which occurs from the incomplete oxidation of oil. Oil is primarily made up of long chains hydrocarbons which on complete combustion (chemical reaction with oxygen), produces carbon dioxide and water. However, most of the reactions that occur in the engines are incomplete, resulting in the production of carboxylic acids along with CO_2 and H_2O. In addition to these reactions, the contaminants present in oil also oxidize and form sulfates, nitrates and formates which further increase the acidity of the oil (Andrews, Xu et al., 2001).

Other factors such as the type of engine, engine oil, driving conditions such as driving in traffic, bumpy roads and on highways also contribute to oil degradation. Accordingly, different techniques and tests have been developed by various research groups to determine the influence of such factors on the extent of oil degradation. For example, researchers at Delphi Automotive Systems tested the TAN change in SAE 5W-30 grade engine oil in Chevrolet under general service and city driving conditions using platinum electrodes (Wang, 2002). Though both the driving conditions showed an increase in the TAN values with mileage, the initial stages or Stage-1 degradation due to depletion of detergents or antioxidants was rapid for city driving conditions. Addition of fresh oil in both the cases showed a decrease in the value of TAN, which was due to the replenishment of detergents to the oil (Wang, 2001; Wang, 2002).

Metals such as iron, chromium, lead and aluminum are used in various moving parts such as piston rings, crankshafts, cylinder liners and bearings. On prolonged usage, they wear to form debris, resulting in the accumulation of these metal particles in the oil.

20

They in turn catalyze the oxidation of oil further increasing the TAN (Andrews et al., 2001). Automobiles are equipped with recyclers to filter out the worn out metal particles and infrared heaters to vaporize the water present in oil, to prevent its reaction with sulphur oxides to form sulfuric acid that further degrades the oil quality. The formation of oxidative products along with the accumulation of worn out metal particles results in the formation of thick black gel in the engine oil known as 'sludge'. **Figure 2.8** depicts such a sludge formed in BMW engine. This sludge increases the engine load and stress by reducing the circulation of oil through the moving parts and preventing the heat exchange to keep the temperature of radiator low. Thus, the gas mileage of the automobile is greatly reduced by the sludge formation which presses on the need for designing better lubricating fluids or synthesizing additives which prevent the sludge formation.
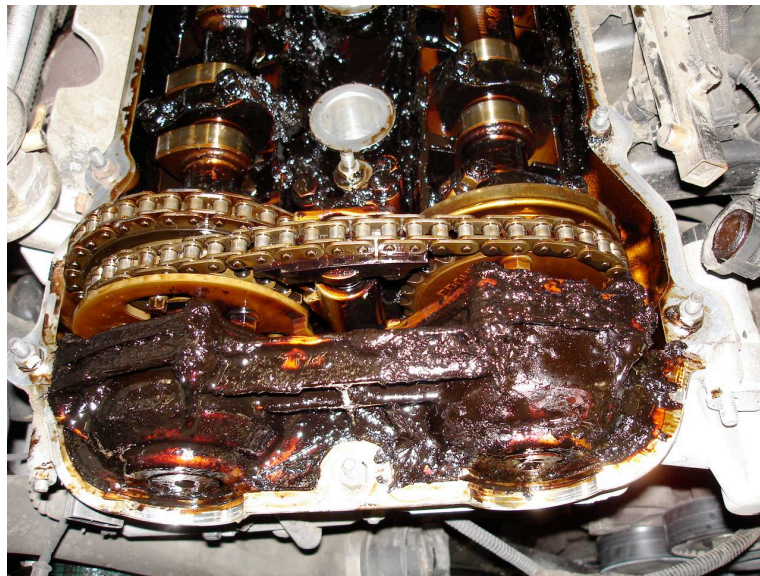
Figure 2.8: Sludge formation in a BMW engine, Photo by M. Kline (Schleeter and McCalmont, 2005)

2.4.3 Survey of current technologies

There are a number of techniques which are used to quantify the change in the acid content of oil. The standard approach involves the use of a titration method approved by *American Society for Testing and Materials* (ASTM) in which the oil sample is dissolved in a solvent and titrated against a base. There are several other techniques that are based on electrical conductivity or electrochemical response (potential) which indirectly measures the TAN. Analogously, Total Base Number (TBN) can be measured using titration methods, which determine the level of alkalinity of the oil or the ability to neutralize acids present in the oil. The ASTM methods for determining TAN are described below (Coverdell, 2007).

2.4.3.1 Total Acid Number (TAN) by ASTM:

a.   **ASTM D974:** The TAN defined by this standard is the milligrams of potassium hydroxide needed to neutralize the acids present in 1 g of oil. It is a colorimetric based titration in which a known volume of oil is dissolved in toluene, p-naphtholbenzene, isopropyl alcohol and water. This dissolved oil is titrated against a known concentration of KOH and at the end point, when the color changes, TAN is determined by the volume of KOH consumed for titration. This method cannot be applied for oil samples that are dark as the color change is undetectable.

b.   **ASTM D664:** This is a potentiometric based titration used in cases where oil samples to be tested are too dark and show no appreciable change in color on

titration using ASTM D974 methos. As an alternative, change in electrochemical response measured by the potentiometer is used for the calculation of TAN.

c.   **ASTM D1534:** This test is similar to the above mentioned ASTM D974. However, it is used to measure TAN for electrically insulating oils having a viscosity not greater than 24cSt at 40°C

d.   **ASTM D3339:** This test is also similar to ASTM D974 but is designed to measure on small oil samples of around 2.0 g.

2.4.3.2 Industrial equipment for TAN/TBN measurement

Several commercial testing kits are available which are able to determine laboratory and on-site measurement of TAN/TBN. Some of these kits are described in the following sections.

a   **Kittiwake™ (UK):** It offers an on-site electronic measurement of TAN/TBN and several other parameters like water content in oil and viscosity. This technique can measure the TAN values from 0 to 6 with an accuracy of ±0.3 TAN and TBN values from 5 to 80 with an accuracy of ±10% TBN (Kittiwake, 2009) **(Figure 2.9).**

Figure 2.9: TAN and TBN testing kits from Kittiwake (Kittiwake, 2009)

a.   **Polaris laboratories™, LLC:** They use a potentiometric titrator for laboratory measurement of TBN and TAN. The results are reported in milligrams potassium hydroxide per gram of sample based on the ASTM method of D4739 which is an alternative to ASTM D664. This method is independent of color or other properties of the oil **(Figure 2.10)** (2009)
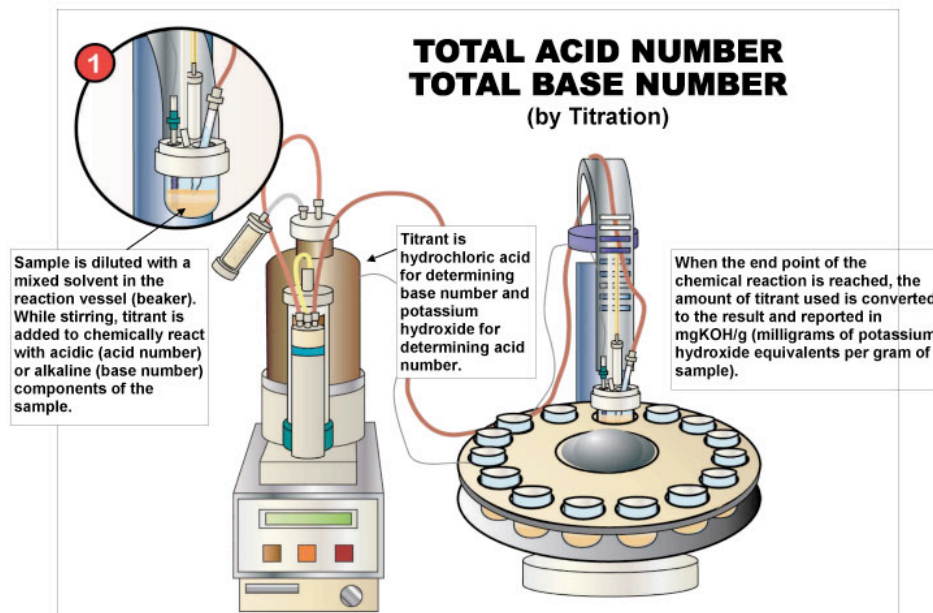
Figure 2.10: Sketch of the potentiometric titrator for measuring TAN from Polaris labs, LLC

(2009)

b.   **Koehler Instrument's™ Automatic Potentiometric Titrator (APT®):** They offer a laboratory based ASTM D664 method of potentiometric titrator equipped with a glass pH electrode for the determination of TAN and TBN. This instrument was used in determining TAN values in this work and its description is mentioned in later section.

2.4.3.3 pH sensing electrodes

The acid content, given by the TAN is a measure of the hydrogen ion concentration in the oils, which is also expressed in terms of pH. Many commercially

available pH-sensing electrodes are used to measure the hydrogen ion concentration (Sheng, Min et al., 2001; Shervedani, Mehrdjardi et al., 2007). These ion selective electrodes operate on the potentiometric determination of cell voltage, also known as Open Circuit Potential (OCP), derived by the Nernst equation. The OCPs are usually measured against standard reference electrodes like Ag/AgCl (3M KCl) and Calomel (Hg/Hg_2Cl_2) using a high impedance (around 20-1000 MΩ) potentiometer.

2.4.3.4 Glass electrodes

Glass electrodes are the most commonly used conventional pH sensing electrodes for laboratory and field measurements of hydrogen ion concentration. These glass electrodes are composed of a network of oxygen atoms or ions held together by silicon atoms in irregular chains (Zachariasen, 1932). The exchange of alkali-metal ions in the glass matrix for the hydrogen ions in the solution was believed to be the reason behind their pH sensing mechanism (Perley, 1949). This mechanism for pH sensing mechanism of glass electrodes was corrected by K. L. Cheng, who suggested that there are two kinds of potentiometric mechanisms – Faradic and Non-Faradic potentiometry. According to him, the latter one explains the pH sensing mechanism in glass electrode (Cheng, 2002). According to his theory, a capacitance potential is developed by the adsorption of charged species such as hydrogen ions (H^+) on the surface of a dielectric or semiconducting material like glass. The OCP on the surface of the glass electrode is calculated by the modified Boltzmann Equation (Eq 1) (Cheng, 1998).

$$E = 0.059 \log(N_i / N_o) \tag{EQ-1}$$

Where, N_i is the number of ions (H^+) or charged particles on the glass electrode surface and N_o is the ionic concentration in the bulk solution.

Due to intrinsic brittle nature of glass membrane, these electrodes are not suitable for rough or in vivo applications. It is also difficult to planarize and miniaturize the glass electrode so that they can be molded into different shapes, sizes and integrated into devices. Thus, researchers have tried to explore alternative materials for pH sensing applications which have good sensitivity as well as offer a scope for miniaturization and planarization.

2.4.3.5 Metal oxide electrodes

Metal oxide based pH electrodes offer the advantages of having greater strength and good sensitivity. They can also be molded, planarized and miniaturized into different shapes which can be integrated to various devices. Since these electrodes are not made of glass, they can endure extreme environments pH sensing properties of metal oxides such as PtO_2, IrO_2, RuO_2, OsO_2, Ta_2O_5 and TiO_2 were reported to exhibit a near Nernstian behavior (Fog et al., 1984) in which the sensitivities varied from 46-68 mV/pH. The redox equilibrium between a higher (*ox*) and a lower valence oxide phase (*red*) was considered to be the governing principle behind the pH sensing mechanism of these metal-oxide electrodes (EQ-2).

$$ox + H^+ + e^- \leftrightarrow red \qquad\qquad \text{(EQ-2)}$$

Hence, according to the Nernst equation given below,

$$E = E_0 + 2.3\frac{RT}{nF}\log\left(\frac{[red]}{[ox]}\right) + 0.059\ln[a_{H^+}] \qquad\qquad \text{(EQ-3)}$$

the Open Circuit Potential (OCP) or the cell potential of the above reaction measured against a standard reference electrode is directly proportional to the concentration of hydrogen ions (EQ-3) in the solution with a slope factor (or pH sensitivity) of 59mV/pH.

Much interest has been shown over the past 20 years in developing iridium oxide based sensors using techniques such as thermal decomposition (Ardizzone, Carugati et al., 1981; Sheng et al., 2001; Wang, Yao et al., 2002) reactive sputtering (Katsube, Lauks et al., 1981) electrochemical oxidation (Burke, Mulcahy et al., 1984; Hitchman and Ramanathan, 1988), pulse deposition (Olthuis, Robben et al., 1990) and anodic deposition (Yamanaka, 1989; Marzouk, 2003). The iridium oxide films synthesized by these methods have both Nernstian and Super-Nernstian behavior depending on the state of hydration of the films (Pásztor, Sekiguchi et al., 1993). The redox reaction in the sputtered iridium oxide films (SIROFs) is given by the EQ-4 in which one electron takes part in the chemical reaction with one hydrogen ion. According to the Nernst equation (EQ-3), a sensitivity of 59mV/pH is obtained and is consistent with the slopes reported by SIROFs (Lauks, Yuen et al., 1983).

$$IrO_2 + H^+ + e^- \leftrightarrow IrOOH \qquad\qquad (EQ\text{-}4)$$

However, the preparation methods involving electro-oxidation by potential cycling (Burke et al., 1984), pulse-oxidation (Olthuis et al., 1990) and anodic electrodeposition (Marzouk, 2003) produce oxyhydroxylated iridium oxide films in which there is more than one hydrogen ion involved per electron in the redox reaction (EQ-5).

$$2Ir(OH)_2O^- + H_2O \leftrightarrow IrO_2(OH)_3O_3^{3-} + 3H^+ + 2e^- \qquad (EQ\text{-}5)$$
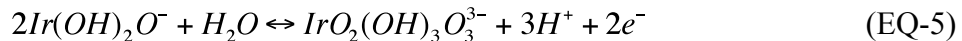
According to the above equation, there are 1.5 hydrogen ions involved per electron in the redox reaction, which gives a sensitivity of 88.5mV/pH according to the Nernst Equation. But in reality, the surface of the electrode is partly oxyhydroxylated giving an intermediate sensitivity around 65-80 mV/pH (Pásztor et al., 1993)

2.4.4 Potentiometric titration

In the automobile industry, the usage of Total Acid Number (TAN) is more prevalent than the 'term pH', though both the terms give a measure of the hydrogen ions present in the oil. In this work, *Koehler Instrument's* Potentiometric Titrator (AT-610) **(Figure 2.11)** was used to calculate the TAN number in the fresh and artificially aged oils. The titration was based on the ASTM method D664 in which a known weight of the oil sample dissolved in a solvent was titrated against a base, potassium hydroxide (KOH). Glass electrode was used as pH sensing electrode and its open circuit potential decreased

29

continuously as the titration progressed. This was expected because as the basicity increases, the potential of the glass electrode decreases. The end point (EP) was calculated by taking the inflection point on the Potential vs. Titrated volume graph. The TAN was calculated by applying the formula (EQ-6):

$$TAN = \frac{EP \times C \times MW}{S} mg/g$$

(EQ-6)

Where, EP = volume of KOH consumed till end point (ml), C = Concentration of KOH (0.1N), MW = Molecular weight of KOH (56.1), S = Sample volume (g)

Figure 2.11: Automatic Potentiometric Titrator by Koehler Instruments

2.4.5 Detection of paraoxon – an application for pH sensing

Paraoxon is a class of P-O bonded organophosphorus (OP) compound which is used as pesticides and insecticides. The annual production of OPs in the United States is over 60 million pounds and 17 million pounds from the agricultural and non-agricultural sectors (http://www.epa.gov/pesticides/op/primer.htm). The exposure of OPs leads to inhibition of acetylcholine enzyme which results in the accumulation of acetylcholine at the end of neuron/neuron and neuron/muscle junctions(Senannayake and Karalliedde, 1987). This results in headache, nausea, abdominal cramps and twitching of muscles. Prolonged or acute exposure of OPs also leads to genetic diseases, cancer and Organophosphate Induced Delayed Neuropathy (OPIDN) (Johnson, 1975), in which the distal degeneration of sensory and motor axons occur and hence it is very important to detect paraoxon in the initial stages of exposure.

Organophosphorus Hydrolase (OPH) is a 72 KDa molecular weight dimeric metalloenzyme which with two zinc ions present at the active site that has catalytic and structural functions (Lai, Dave et al., 1994). Paraoxon undergoes rapid hydrolysis in the presence of OPH, giving diethyl phosphate and para-nitro phenol and two protons (Lewis, Donarski et al., 1988). Accordingly, many OPH-based biosensors have been developed to detect paraoxon by measuring the micrenvironmental changes in pH resulting from catalytic hydrolysis (Viveros, Paliwal et al.; Simonian, Rainina et al., 1997; Simonian, Efremenko et al., 2001; Viveros, Paliwal et al., 2006; Ramanathan and Simonian, 2007).

2.4.6 Current work

In this study, formation of iridium oxide films by anodic electrodeposition on titanium substrates and by electrochemical oxidation of iridium wire were done for measuring pH in aqueous and non-aqueous solutions (oils). The TAN values were obtained from the Automatic Potentiometric Titrator whose trend was in accordance with the Open Circuit Potentials (OCPs) obtained from the iridium oxide pH sensitive electrodes.

This mechanism of pH sensing was applied for the detection of Paraoxon, an organophosphorus compound. Paraoxon hydrolyzes in the presence of the enzyme OPH giving two protons per molecule there by decreasing the pH of the solution. This change in pH was detected by the iridium oxide films coated on the inside walls of the titanium tubes. A multi-channel pH sensor was fabricated using a PDMS block on enzyme immobilized glass slide coated with titanium oxide nanoparticles.

CHAPTER 3

MATERIALS AND METHODS

3.1 Objectives

The objectives of the study involving the development of a sensor for Tricresyl phosphate (TCP) detection are as follows:

- Develop a hydrolyzing medium for the degradation of non-electroactive TCP to electro-active cresols

- Develop a sensitive electrode to detect cresols resulting from TCP hydrolysis

- Integrate the hydrolyzing column, sensing electrode and potentiostat to develop a compact, automated and portable TCP sensing unit that is simple to operate by the flight attendants on board

The objectives of the study involving the development of a sensor for the determination of acid content in engine oil are as follows:

- Fabricate a pH sensitive iridium oxide coated titanium electrode by galvanostatic deposition of iridium oxalate solution

- Determine the Total Acid Number (TAN) values of artificially aged oils by potentiometric titration

- Create a multi-channel pH sensor using the fabricated iridium oxide-Ti electrode for the detection of paraoxon that undergoes catalytic hydrolysis by Organophosphorus Hydrolase (OPH)

3.2 Materials and methods for TCP detection

3.2.1 Materials

Multi-walled carbon nanotubes were purchased from Nanolabs (Newton, MA), nafion (5 wt% solution in a mixture of lower aliphatic alcohols), concentrated sulfuric acid, concentrated nitric acid and phosphate buffer saline (PBS) were purchased from Sigma-Aldrich (St. Louis, MO), De-ionized (DI) water (Type I Millipore ≤ 18.2MΩ) was used from Millipore water purification system (Billerica, MA), Sodium 3,5 dibromo-4-nitroso benzene sulfonate (DBNBS, F.W. 367, antifouling agent) was obtained from Dr. David Stanbury (department of chemistry, Auburn University), sodium sulfate (ACS grade, F.W. 142.04) was purchased from Fisher Scientific (Pittsburg, PA), tricresyl phosphate (99.2%, F.W. 344) was purchased from Chem Service (West Chester, PA), ortho cresol (99+%, F.W. 108.14) was purchased from Acros Organics (Morris Plains, NJ) and α-alumina slurries (1, 0.3 and 0.05 μm) were purchased from Buehler (Lake Bluff, IL).

Potentiostat (model 910B) was purchased from CH Instruments (Austin, TX), glassy carbon electrodes and Ag/AgCl (3M KCl) electrode were purchased from BASi Inc. (West Lafayette, IN), platinum wire (Ø=0.404 mm) was purchased from Alfa Aesar (Ward Hill, MA), ISMATIC peristaltic pump was purchased from IDEX Corporation (Northbrook, IL), 12 port injection system was purchased from Valco Instruments Co

(Houston, TX), ultrasonicator (PN 1510) was purchased from Branson (Danbury, CT), Personal Measurement Device (PMD 1608 FS) was purchased from Measurement and Computing (Norton, MA), reed relays (ELEC-TROL R1947-2) were purchased from Surplus Sales of Nebraska (Omaha, NE).

3.2.2 Instrumentation

3.2.2.1 Potentiostat

The potentiostat used in this study was purchased from CH Instruments (Model CHI 910B) and has been widely used for performing various electrochemical techniques such voltammetry, amperometry and potentiometry in addition to surface characterization studies, as it was described in (Bard et al., 1989, Wei, et al., 1995, Anthony et al., 2008). **Figure 3.1** shows the set up of the potentiostat instrument used in the current study
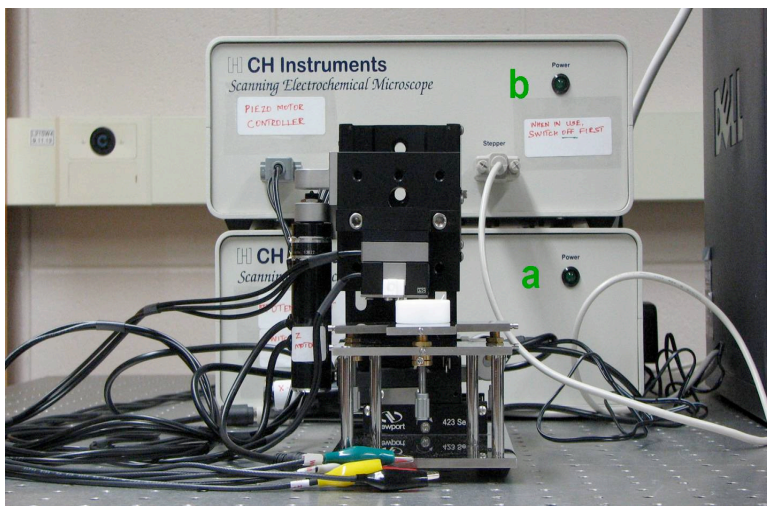
Figure 3.1: CH Instruments™ Potentiostat

The four electrode leads coming out of the potentiostat are differentiated by the color of the insulation on their alligator clips. Green and yellow leads are the working electrodes, red and white leads are the auxiliary and reference electrodes respectively.

3.2.3 Electrodes used for detection

3.2.3.1 Working electrode

Glassy carbon (GC) electrode was purchased from BASi™ to serve as the working electrode. The electrode used for batch mode experiments had a 3 mm diameter glassy carbon rod embedded inside an insulating material of length 7.5 cm. One end of the electrode had a smooth, shiny glassy carbon surface and the other end had a gold pin for electrical contact **(Figure 3.2).** In the case of flow based measurements, a 2 mm diameter glassy carbon rod was embedded inside an insulating material to serve as the working electrode **(Figure 3.3**). Prior to performing any voltammetric or amperometric studies, the electrode was polished over 1, 0.3 and 0.05 μm α-alumina slurries. After polishing, the electrode was sonicated (Branson™ ultrasonicator) in ethanol for 5 minutes and dried under nitrogen atmosphere. The glassy carbon electrodes thus prepared will be referred to as un-modified electrodes.
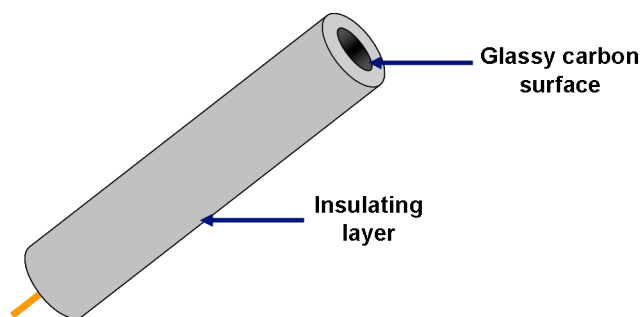
Figure 3.2: Glassy carbon working electrode for batch mode experiments
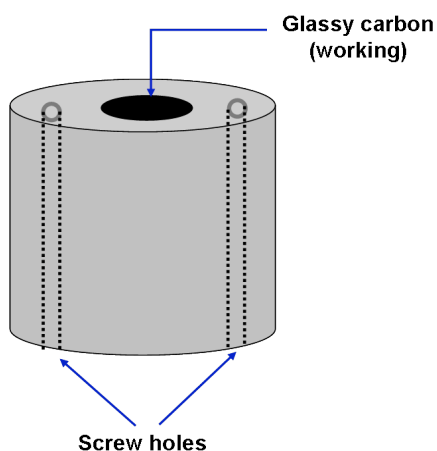
Figure 3.3: Glassy carbon working electrode for flow based experiments

3.2.3.2 Modification of working electrode

The working electrode that was made of glass carbon (GC) was modified using different methods and their sensing characteristics were compared. The first modification involved the use of multi-walled carbon nanotubes on GC while the second modification involved copper nanoparticles deposition on multi-walled nanotubes. The method used for modification is detailed below.

37

a. Preparation of Multi-walled carbon nanotubes modified GC electrodes

Multi-walled carbon nanotubes (MWCNT, 95% purity) were obtained commercially from Nanolabs™. These nanotubes were 1 to 5μm long with a diameter of 30±10nm. 2 mg of these nanotubes were mixed with a 3:1 ratio of concentrated nitric and concentrated sulfuric acid respectively. A suspension of these nanotubes was sonicated at room temperature in the Branson™ sonicator for 10 hours. After sonication, the contents of this solution were filtered using centrifugation and a filter paper. The supernatant of this filtration was discarded and the nanotube filtrate obtained was continuously washed with DI water until the pH of the solution was neutral. After washing, the DI water was drained out and the nanotubes were dispersed in 1:1 ratio of nanotubes and 0.5% nafion solution. 5μl and 3μl of this dispersed solution were cast on the batch mode and flow mode GC electrodes respectively. These electrodes were allowed to dry under room temperature conditions before they can be used for voltammetric or amperometric studies (**Figure 3.4**).
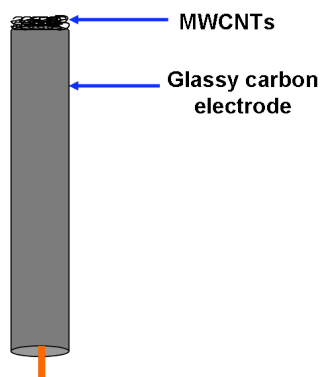
Figure 3.4: MWCNT modified glassy carbon electrode

b. Copper nanoparticle deposition on GC/ MWCNTs

Copper was deposited onto the GC modified with MWCNTs by amperometric method. 0.1M sodium sulfate (Na_2SO_4) with 2mM copper sulfate ($CuSO_4$) formed the deposition solution. The glassy carbon modified with MWCNTs, platinum wire and Ag/AgCl (3M KCl) was used as the working, auxiliary and reference electrodes respectively A potential of -1V was applied against the Ag/AgCl (3M KCl) reference electrode for varying times to observe the extent of copper deposited on the carbon nanotubes **(Figure 3.5)**..
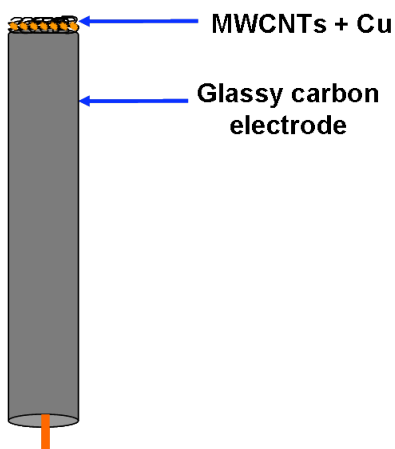
Figure 3.5: Copper deposited on MWCNT modified glassy carbon electrode

3.2.3.3. Auxiliary and reference electrodes

Platinum wire of diameter Ø=0.404 mm was used as the auxiliary electrode and a silver-silver chloride (Ag/AgCl) with 3 M KCl internal solution was used as the reference electrode for batch mode experiments. The platinum wire was polished gently with 1500 grade emery paper, rinsed thoroughly in DI water and dried before use. The reference

electrode was rinsed in DI water before every measurement. When not in use, the reference electrode was stored in 3 M KCl solution.

A flow block purchased from BASi, was used for flow based experiments. This block consisted of 2 parts that could be screwed onto one another. One of the blocks had the working electrode consisting of modified GC electrodes. The complementary block had stainless steel (Ø=2mm) and saturated Ag/AgCl (Ø=1mm) in the form of circular discs to serve as the auxiliary and reference electrodes respectively (**Figure 3.6**). The block was rinsed in DI water and dried before performing any flow based analysis. This complementary block was screwed onto the block containing the working electrode with a silicone gasket sandwiched in between them forming a flow cell **(Figure 3.7)**. The fluid flowing through the flow block was in continuous contact with all the three (working, auxiliary and reference) electrodes.
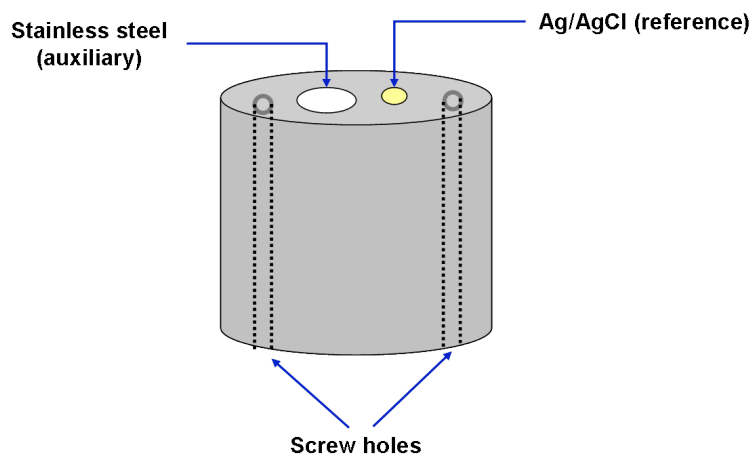
Figure 3.6: Auxiliary and reference electrodes for flow mode experiments
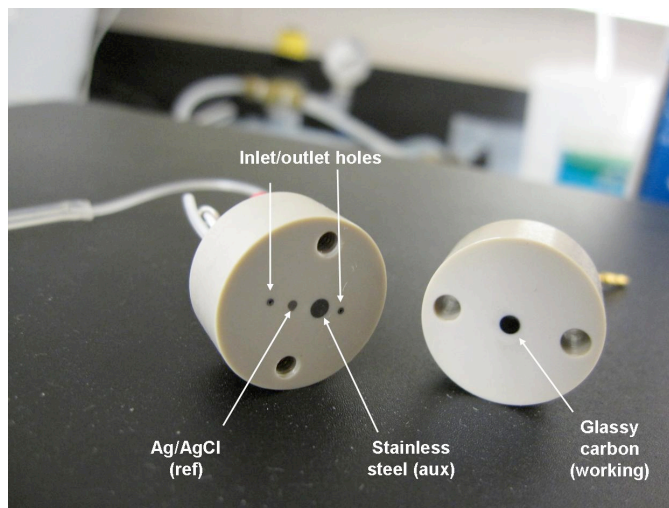
Figure 3.7: The two blocks for flow based analysis: The left has auxiliary and reference and the right has the working electrode

3.2.4 Hydrolyzing media

Alumina powder (Al_2O_3) modified with sodium hydroxide was used as a basic support for TCP hydrolysis. This media was optimized by testing on mixtures containing various weight ratios of sodium hydroxide pellets and alumina. DI water was added to the above mixture and stirred continuously to obtain a uniform slurry. This slurry was kept in a vacuum chamber for 3-4 hours until all the water evaporated resulting in a free flowing final powder. 100 mg of this powder was packed into a column with filter papers on either ends to contain the particles inside the column **(Figure 3.8)**. This column was fitted to 1/8 inch silicone tubes on either ends to enable flow based analysis.

41
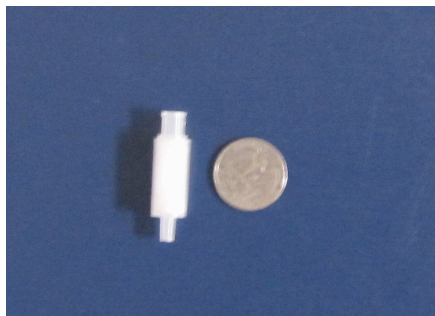
Figure 3.8 Hydrolyzing column containing alumina particles modified with sodium hydroxide (size compared with a US quarter dollar)

3.2.5 DBNBS reagent

Sodium 3,5 dibromo-4-nitroso benzene sulfonate **(Figure 3.9)**, commonly known as DBNBS reagent was used for scavenging the oxidized cresol radicals that may form on the electrode surface. A stock solution of 1M concentration of this reagent was made by dissolving in DI water. 1:1 ratio of this reagent and o-cresol were used to determine the fouling effects of oxidation of o-cresol on the surface of the glassy carbon electrode.
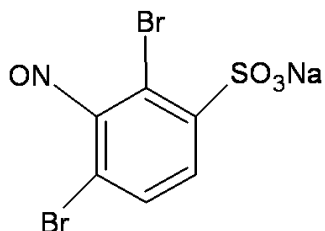
Figure 3.9: Structure of DBNBS reagent

3.2.6 Experimental Procedures

3.2.6.1 Batch mode measurements

Voltammetry (cyclic (CV) and linear sweep (LSV)) and amperometry studies were performed for batch mode experiments. A 20 ml cylindrical glass beaker containing the sample solution was provided with a removable 4-hole plastic cap to hold the three electrodes **(Figure 3.10)**. The fourth hole in the cap allowed the injection of sample. It was ensured that all the three electrodes were in contact with the solution and not touching each other at the same time.
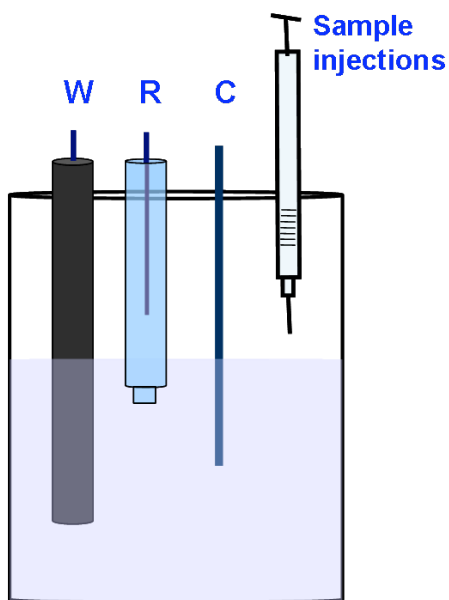
Figure 3.10: Three electrode cell for batch mode experiments: W: Working electrode, R: reference electrode, C: auxiliary

O-cresols were used as the target analyte for preliminary studies to characterize the sensing properties of prepared GC modified electrodes. Various concentrations of o-cresols were formulated in 5 ml of 10 mM PBS buffer, pH 7.4.

CVs and LSVs were obtained for various concentrations of o-cresols (2 μM, 20 μM, 40 μM and 100 μM) by applying a potential between 100mV and 900mV at a scan rate of 50mVs^{-1}.

In amperometric measurements, different voltages were selected for GC and GC electrodes modified with MWCNTs and Cu deposited MWCNTs. 0.7 V was applied for GC and GC/MWCNT electrodes while 0.54 V was applied for GC/MWCNT-Cu electrodes. Cresol samples were added during the amperometric measurements via the fourth hole drilled in the plastic cap of the beaker. Time of operation was set to a default value of 10 minutes for all the measurements.

3.2.6.2 Flow based measurements

The flow based setup consists of three important components: Peristaltic device, 12 port flow injection system and a three electrode flow injection electrochemical cell made of two blocks screwed together **(Figure 3.11).** Peristaltic pump manufactured by ISMATEC™ was used to run the buffer at a flow rate of 1ml/min through the system. The 12 port flow injection system was used to flow buffer and sample to the three electrode flow cell. Cresol was contained in the syringe as shown in the **Figure 3.11**. The knob of the 12 port flow injection system was turned either clockwise or anticlockwise to allow the injection of cresol samples into the electrochemical cell.
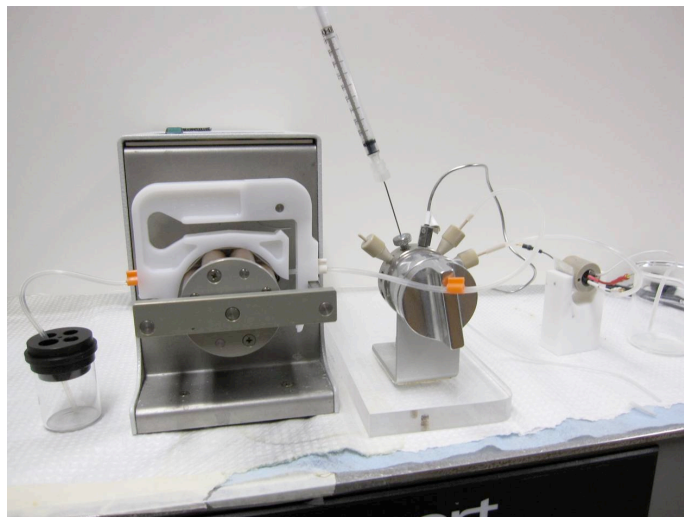
Figure 3.11: Experimental setup for flow based amperometry. The 12 port injection value by Valco™ connected to the peristaltic pump on the left and the three electrode cell on the right.

3.2.7 Detection in air and automation

3.2.7.1 Setup for detection in air

Unlike o-cresols used in preliminary experiments, TCP was used to test the sensor for air-samples. TCP is usually obtained as a liquid from the manufacturer. Initial experiments were conducted by injecting the TCP in liquid form into the hydrolyzing column. In the case of TCP detection in air, its vapors were made to enter the hydrolyzing column.

Automation was done to miniaturize the system, make the sensor portable for on-site detection and simplify its operation to allow its use by non-technical personnel. To

develop such an automated system, LabVIEW® software was used for controlling the processes such as obtaining cresols from the TCP column, injecting the cresols to the electrochemical cell and finally washing the electrode surface with DI water. The schematic of setup for automization is shown the **Figure 3.12.**
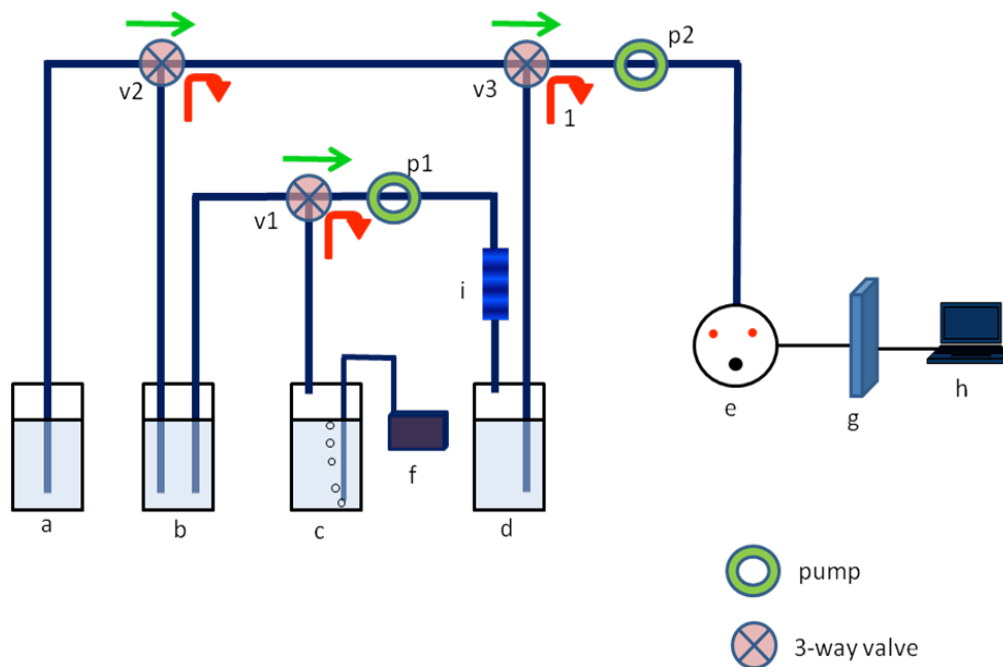
Figure 3.12: Schematic of the automization of the sensor for detection of TCP in air samples

Containers (a) and (b) in the **Figure 3.12** represent 100 ml glass beakers containing 50 ml of DI water and 10mM PBS buffer, pH 7.4 respectively. They can thus be referred as the water and buffer reservoirs. 20 mM TCP dissolved in methanol is present in beaker (c), which is a 20 ml glass bottle with an airtight cap. The beaker (d) is an empty 10ml plastic bottle that is used to collect the cresols resulting from TCP hydrolysis upon reaction with alumina hydrolyzing column represented as (i). An

aquarium pump (f) was used to bubble the TCP solution in beaker (c). Care was taken to ensure that the cap maintained a good seal in beaker (c) to avoid exposure to TCP vapors. The tubing diagram connecting the beakers, TCP hydrolyzing column (i) and the electrochemical cell (e) is shown in the figure. In the schematic, the concentric green circles represent peristaltic pumps (p1 & p2) by Instech™ and the pink colored circle with a cross represent the three way valves (v1, v2 & v3) by LEE Co™. 18V and 5V dc power supplies were used to power the pumps and valves respectively. The peristaltic pumps were connected in such a way that the fluid was drawn towards the hydrolyzing column for pump, p1 and towards the electrochemical cell for pump, p2. The speed of the pumps were adjusted by turning a screw on the pump circuit and was set to deliver a flow rate of 1 ml/min. The three way valves allow the fluid to flow in a particular direction depending on the voltage applied to it. Red arrow corresponds to direction of fluid when no voltage is applied and green arrow directs the flow when a minimum of 3V is supplied to it. The working, auxiliary and reference electrodes of the flow based electrochemical cell were connected to the potentiostat (g). The current response was read from a laptop or a desktop connected to the potentiostat. The working electrode used in the electrochemical cell was GC/MWCNT-Cu and a potential of 0.54V *vs.* Ag/AgCl (3 M KCl) was applied to it.

The pumps and valves were controlled by a Personal Measurement Device (PMD 1608 FS) through a code developed in LabVIEW®. According to the code, the user was asked to enter the duration (in seconds) of various processes such as obtaining cresols from TCP hydrolyzed column, injecting the cresols to the electrochemical cell and

washing the cell with DI water. The front panel of the LabVIEW program where the time durations were entered is shown in **Figure 3.13**. Upon executing the code, all the fluid transport processes were run automatically by the two pumps p1, p2 and the three valves v1, v2 & v3.
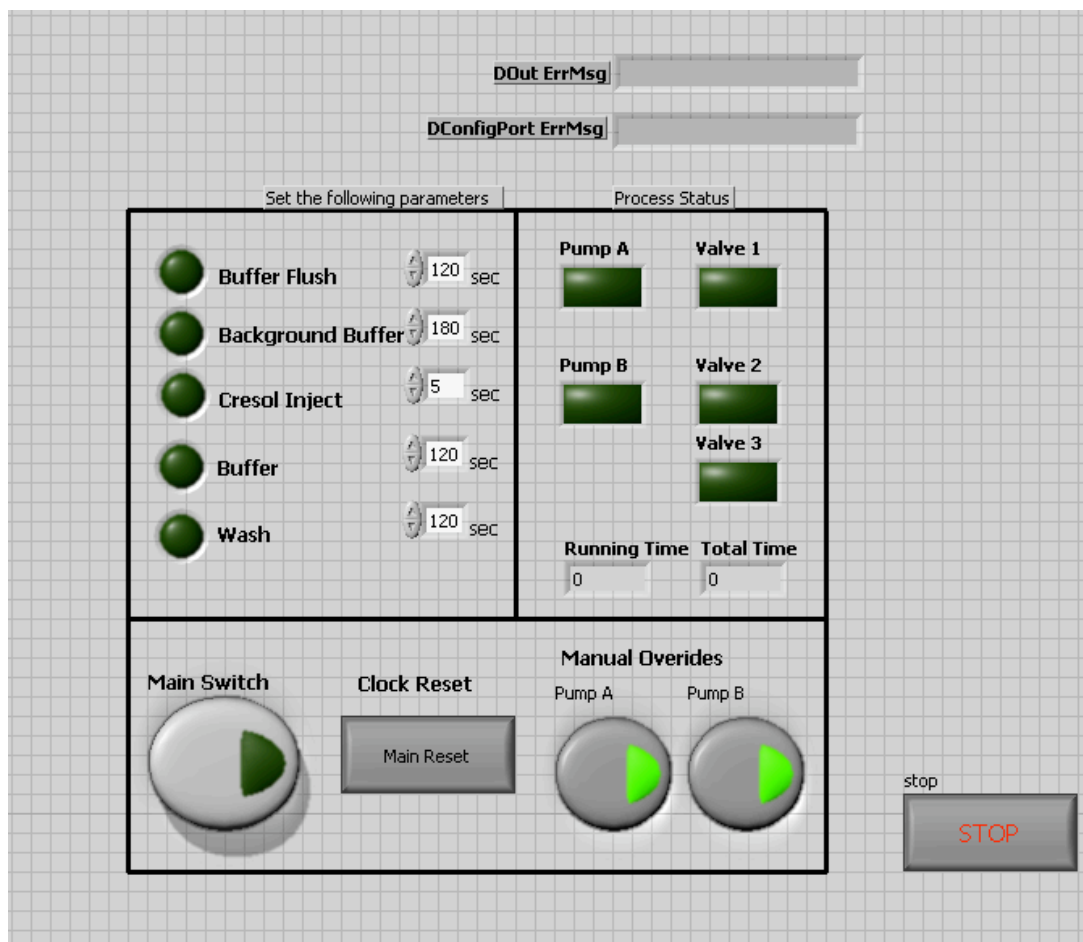
Figure 3.13: Front panel of the LabVIEW® program

3.2.7.2 Process sequence automation

Before the automation was started, the aquarium pump was turned on, which forced the TCP vapors to flow from the beaker (c) to the hydrolyzing column (i) for 15

48

minutes. By default, the valve v1 was in off position. At the end of 15 minutes, the TCP solution was completely vaporized and was adsorbed onto the modified alumina particles in the hydrolyzing column. Now the automation program was run, which turned on the pump p1 and valve v1 such that 5 ml buffer was allowed to pass from the bottle (b) to the beaker (d) flushing all the hydrolyzed contents through the column. According to the code, p1 was stopped and p2 was turned on keeping the valves v2 and v3 turned off which enabled the buffer to flow from bottle (b) to the electrochemical cell (e). At this point the amperometric technique was kept running, maintaining the potential of the working electrode at 0.54V against Ag/AgCl reference electrode. This was continued for 5 minutes until a stable background current was obtained from the amperometric detection. After this, the valve v3 was quickly turned off and on, such that only 50μl of cresols from beaker (d) were injected into the main stream of buffer. This 50μl cresol sample on reaching the electrochemical cell, oxidized, producing a response current. The height of the peak was used to determine the concentration of cresol resulting from hydrolysis. Multiple injections can be used in which 50μl of cresol samples were injected into the main streams to study the effect of fouling on the surface of the electrode.

3.3 Materials and methods for determination of acid content in oils

3.3.1 Materials

3.3.1.1 Materials for determination of acid content in oils

Iridium (IV) chloride (99.95%), titanium foil (thickness=0.89mm), titanium rod (99.7%, ∅=2mm) and potassium oxalate monohydrate (99%) were purchased from Alfa

Aesar (Ward Hill, MA), hydrogen peroxide (30%), potassium chloride, potassium carbonate (F.W. 165.24) and concentrated sulfuric acid were purchased from Fisher Scientific (Pittsburgh, PA).

Electrical Discharging Machining (EDM, Model HS 300) by Brother International Corporation (Bridgewater, NJ) was used from the department of materials engineering, Auburn University, Ultrasonicator (PN 1510) was purchased from Branson (Danbury, CT), Potentiostat (model 910B) was purchased from CH Instruments (Austin, TX), Automatic Potentiometric Titrator (Model No. KEM AT-610) was purchased from Koehler Instruments (Bohemia, NY).

3.3.1.2 Materials for paraoxon detection

Ti-nanoxide T paste was purchased from Solaronix (Aubonne, Switzerland), absolute ethyl alcohol was purchased from Florida Distillers (Lake Alfred, FL), anhydrous toulene was purchased from EMD (Gibbstown, NJ), *N-_-* maleimidobutyryloxy succinimide ester (GMBS) and neutravidin (biotin binding protein) were purchased from Pierce (Rockford, IL), biotin-XXSE ((2-[*N*-cyclohexylamino] ethanesul 6 ((6 ((biotinoyl) amino) hexanoyl) amino) hexanoic acid) succinimidyl ester) was purchased from Molecular Probes (Carlsbad, CA), glass slides, standard pH buffers (4.00, 7.00 & 10.00) were purchased from VWR Scientific (West Chester, PA), nitrogen gas (Ultra High Purity) was purchased from Airgas Inc South (Atlanta, GA), wild-type OPH (E.C.3.1.8.1) isolated from recombinant Escherichia coli strain was obtained from Texas A&M (Dr. James Wild's Lab), paraoxon (diethyl-p-nitro phenyl phosphate, FW. 275.22) was obtained from Chem Service (West Chester, PA). dimethyl sulfoxide

(DMSO), phosphate buffer, Bovine Serum Albumin (BSA, Fract V, cold alcohol precipitated), 1 N hydrochloric Acid and 3-(mercaptopropyl)-trimethoxysilane (MPTS) were purchased from Sigma-Aldrich (St. Louis, MO).

Personal Measurement Device (PMD 1608 FS) was purchased from Measurement and Computing (Norton, MA) and ISMATIC peristaltic pump was purchased from IDEX Corporation (Northbrook, IL).

DI water (Type I Millipore $\leq 18.2M\Omega$) for making the solutions was obtained from Millipore water purification system (Billerica, MA).

3.3.2 Preparation of working electrodes

Titanium metal in the form of foil, rods and tubes was chosen to be the substrate for the deposition of iridium oxide. The foil which was originally received from the company, Alfa Aesar™ was cut in to the shape shown in the **Figure 3.14** using Electrical Discharging Machining (EDM) (**Figure 3.15**). The 5x5 mm^2 area was used for electrodeposition while the remaining area served to provide for electrical connection by soldering a copper wire onto it. The electrical connections were sealed with a heat shrinkable tubing to avoid contact with the solutions.
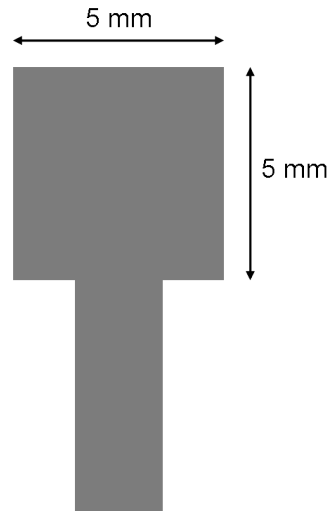
Figure 3.14: Shape of the foil type titanium metal substrate

Figure 3.15: Electrical Discharging Machining (EDM)

Titanium rods of 2 mm in diameter were cut into a length of 2 cm. Heat shrinkable tubing was fitted on to this rod such that it covered the entire rod leaving the cross section on one end for deposition and 4-5 mm on the other end for making electrical connection (**Figure 3.16).**
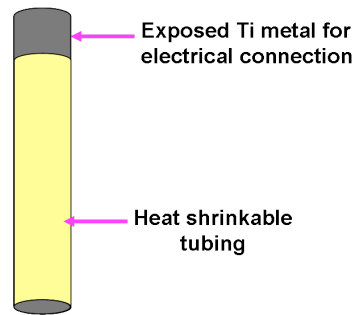
Figure 3.16: Titanium rod with heat shrinkable tubing

In the case of tube electrode, the titanium rod was drilled with a 1 mm stainless steel drill bit to make it hollow such that the inner diameter of the tube was around 1.5 mm **(Figure 3.17)**. No heat shrinkable tubing was fitted on to this type of electrode and the electrical connection was made by simply clamping the tube on its top with alligator clips.
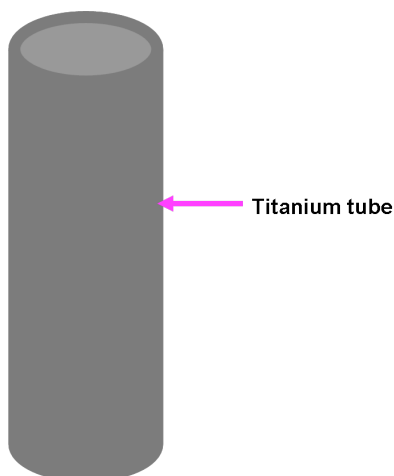
Titanium tube

Figure 3.17: Titanium tube

The electrodes (foil and rod) were polished on a 1500 grade emery paper for 15 minutes and rinsed in DI water. These electrodes were later placed in 70% sulfuric acid at 80°C for 10 minutes to remove any impurities and roughen the surface to enable better adhesion of iridium oxide films (Marzouk, 2003). After the surface etching process with sulfuric acid, the electrodes were thoroughly rinsed in DI water and sonicated in acetone for 10 minutes. Following sonication, the electrodes were dried in air and used immediately for deposition to avoid any contamination with time. All these cleaning methods were also followed for tube electrodes excepting the polishing step involving emery paper.

3.3.3 Preparation of reference electrodes

Silver-silver chloride (Ag/AgCl) with 3M potassium chloride (KCl) internal solution obtained from BASi™ was used as the reference electrode. However, this electrode is not suitable to use in non-aqueous solvents and solutions like oil. Studies

have shown that silver-silver oxide electrodes (Ag/AgO) work well as reference electrodes in oil based systems (Smiechowski et al., 2003).

In this study, approximately 3 cm of silver wire was polished with 1500 grade emery paper, rinsed in DI water and air-dried. This wire was made the anode and a standard Ag/AgCl (3M KCl) electrode was used as cathode. A potential of 1 V in aqueous acetate buffer was applied for 10 minutes. A brown color was observed due to the oxide formation on silver wire. The Ag/AgO reference electrode thus developed, was soldered to a gold connector to make an electrical contact.

3.3.4 Deposition solution

The synthesis route for the deposition solution was originally developed by Yamanaka in 1989 (Yamanaka, 1989), commonly known as Yamanaka procedure. The synthesis method used in this work was a modified Yamanaka procedure (Marzouk, 2003) which was found to be better in terms of film stability (Marzouk, 2003). In this procedure, 75 mg of iridium (IV) chloride was dissolved in 50 ml of DI water and stirred for using a magnetic stirrer. After 10 minutes, 500µl of 30% hydrogen peroxide (H_2O_2) was added and allowed to stir for another 10 minutes. Then 365 mg of potassium oxalate monohydrate was added to this solution and allowed to stir for 10 minutes. The pH of the resulting solution was adjusted to 10.5 using potassium carbonate. The solution was then transferred to a glass bottle, covered with an aluminum foil to avoid exposure to light and stored in a refrigerator at 4°C. This is the deposition solution.

3.3.5 Absorbance studies on the deposition solution

Ultraviolet-visible spectroscopy (UV-Vis) was used to quantitatively determine the presence of organic compounds and transition metal ions in a solution. Iridium being a transition metal, quantitative studies of Ir^{4+} at various stages of the deposition solution preparation can be studied by this method. 2ml samples of the deposition were taken after the dissolution of $IrCl_4$ in DI water, after the pH adjustment step (Day 0) and after 1, 2, 3, 6 & 7 days of preparation of deposition solution. A UV-Visible spectrophotomer (Ultrospec 2100 pro, Amersham Biosciences) was used to obtain wave scans taken between 200 nm and 900 nm and the absorbance was measured on the deposition solutions.

3.3.6 Galvanostatic deposition

Chronopotentiometric technique of the CH Instrument's™ potentiostat was used for the galvanostatic deposition of iridium oxide. Around 20 ml of the deposition solution was brought up to the room temperature. The anode, that was made of titanium substrates (foil, rod and tube) was connected to the green colored insulated alligator clip of the potentiostat. The red colored insulated alligator clip was clamped to a platinum wire (Ø=0.404mm) which served as the cathode. The titanium substrates, connected by the connection cables were made to dip in the deposition solution in such a way that only that area of the electrode was allowed to be in contact with the solution where the deposition was required **(Figure 3.18).** The platinum wire connected by the red color cable was lowered into the solution. Once, the setup was ready, an anodic current density of $2mA/cm^2$ was applied for 180 seconds that resulted in the formation of a dark bluish

layer on the titanium metal. After the deposition, the electrode was carefully removed from the solution and rinsed thoroughly with DI water. This electrode was stored in a pH 7.0 buffer for at least 2 days before it was used.
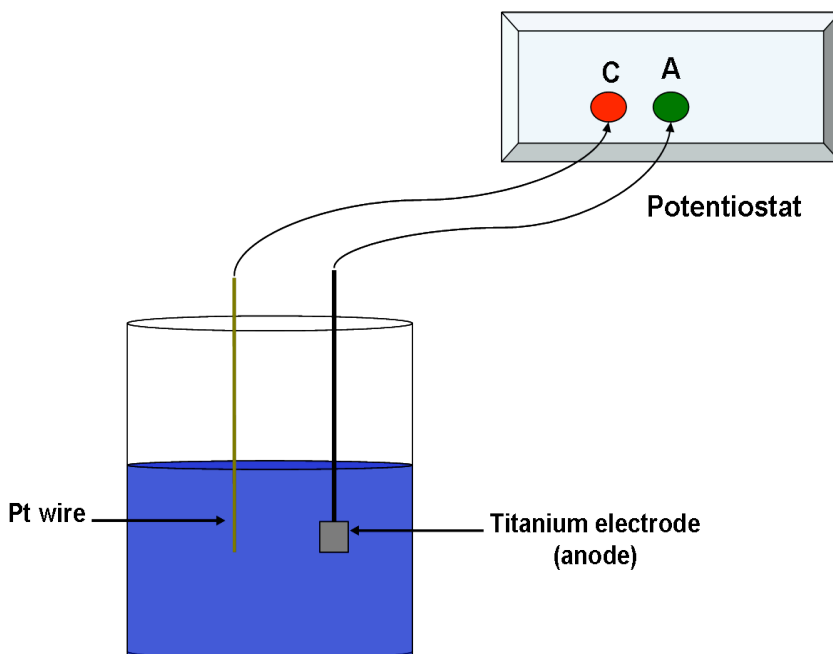
Figure 3.18: Galvanostatic deposition of iridium oxide on titanium foil electrode

3.3.7 OCP measurement

Open Circuit Potential (OCP) is the potential difference measured between two points measured at zero current. In this case, the OCPs were calculated between the pH sensitive iridium oxide coated titanium electrodes and Ag/AgCl (3 M KCl) reference electrodes. In the potentiostat, the green color cable was clamped to the pH sensitive electrode and the white colored cable was clamped to the reference electrode. The data (OCPs) in all the experiments were collected with a sample interval of 0.1 seconds.

OCP was not directly measured in the oil samples because of its high resistivity. The oil was dissolved in a 1:10 volume ratio of oil sample to isopropanol with the help of a magnetic stirrer. The potential difference between the iridium oxide coated titanium electrode and the Ag/AgO reference electrode was measured in the oil-isopropanol mixture.

3.3.8 Artificial aging of oils

Open circuit Potentials (OCPs) from the pH sensitive iridium oxide electrodes and TAN measurements from the Automatic Potentiometric Titrator were determined in fresh and artificially aged oils. The oil used in both the cases was BP Turbo Oil 2197 (BPTO 2380). The artificial aging of the oils were done at the Materials Engineering department, Auburn University, wherein the oil was kept at 150°C in a heat incubation chamber. Samples of this oil were procured after 12, 24, 48 and 96 hours of heat treatment at 150°C.

3.3.9 Automatic Potentiometric Titrator (APT) - Description

Automatic Potentiometric Titrator, APT (Model No. KEM AT-610), that was purchased from Koehler Instruments™ (Bohemia, NY) was used to determine the Total Acid Number (TAN) in fresh and artificially aged oils. This unit consists of 4 major components – Potentiometric unit, Burette unit, Touch-on panel main control and Impact dot printer as shown in **Figure 3.19**.

The figure shows an Automatic Potentiometric Titrator with the following labels: Alcoholic base, Electrode setup, LCD panel, Impact dot printer, Potentiometric unit, Magnetic stirrer. The text box on the image reads:

AT-610 is the highest-end model among the *KEM* Automatic Potentiometric Titrators, featuring an over-sized touch screen LCD to allow for better operations.

In combination with the *KEM* Karl Fischer Moisture Titrator 610 series, the end-user can simultaneously carry out not only a regular titration by AT-610 but moisture titration by the Karl Fischer Moisture Titrator 610 series.

The combination with the optional CHA-600 Sample changer allows for even better operations and laborsaving.

Figure 3.19: Automatic Potentiometric Titrator by Koehler Instruments

3.3.9.1 Burette Unit (PN EBU-610-20B)

The Burette unit consisted of a bottle containing alcoholic base i.e., 0.1 N potassium hydroxide (KOH) dissolved in isopropanol, a piston to inject the alcoholic base from the nozzle to the titration beaker, electrodes to obtain potentiometric data and a magnetic stirrer on which the oil sample was stirred in the titration beaker. The titration solvent in which the oil sample was dissolved was prepared by mixing 500 ml of toluene, 495 ml of isopropyl alcohol (IPA) and 5 ml of DI water. The electrode setup consisted of

a combination glass electrode with an internal Ag/AgCl (3.33M KCl) reference electrode (PN 98-100-C171) and a temperature compensation electrode (PN 98-100-T171) to account for temperature changes. The titration beaker consisted of a 200 ml glass beaker , a magnetic bead that was placed on a magnetic stirrer connected to the potentiometric unit.

3.3.9.2 Potentiometric Unit (AT-610)

The potentiometric unit consisted of an electrochemical analyzer and an automated system to perform various functions like injecting the titration solvent from the Burette unit to the titration beaker, taking functions given by the user on the Touch-on panel and setting different speeds for the magnetic stirrer. The Burette unit is usually placed on top of the potentiometric unit.

3.3.9.3 Touch-on panel main control (PN MCU-610):

This is a high-resolution touch sensitive Liquid Crystal Display (LCD) screen which can be used by the user to enter information to the potentiometric unit and view the real-time results obtained from the titration.

3.3.9.4 Impact dot printer (PN IDB-100-10):

It is a dot matrix printer or impact matrix printer connected to the Touch-on panel used to print the results on a paper obtained at the end of the titration. Only numeric results were obtained here.

3.3.9.5 Settings for potentiometric titration

Before measuring the TAN for oils using potentiometric titration, it is important to calibrate the combination glass electrode with standard pH buffers. "Manual Mode" of calibration was selected on the LCD panel in which the user has to enter three different pH values for which the calibrations need to be done. In the current work, three pH standards (4.01, 7.00 and 10.00) from VWR Scientific™ were used. Purging is an important step before any titration based experiment on the APT. In this step, the alcoholic base, 0.1 N KOH in IPA of 5 ml was purged or disposed through the nozzle into the titration beaker. This step removed all the air bubbles which were present in the nozzle.

3.3.10 Experimental procedure for TAN measurement

10 grams of the oil sample to be tested was weighed in a 250 ml titration beaker and placed over the magnetic stirrer **(Figure 3.19).** 100 ml of the titration solvent and a magnetic stir bar were added to the titration beaker. The electrode holder containing the nozzle from the alcoholic base container, combination glass electrode and temperature compensation electrode were lowered into the beaker touching the dissolved oil sample. The glass electrode and the temperature compensation electrode were initially rinsed thoroughly in DI water and dried to remove any water droplets present on these electrodes. On the LCD panel, "Auto Titration" was selected as the "method name" and "Auto titration (EP stop)" was chosen as the "Titration mode". This setting allowed the alcoholic base to be automatically injected through the nozzle to the titration beaker and once the titration reached its end point, the base injection was automatically stopped. All

the other settings like dosage (amount of 0.1N KOH injected per second), stirrer speed and control speed mode were left unchanged to "Standard mode".

3.4 Application of pH sensing metal oxide electrodes for organophosphates detection

The application of the developed pH sensing metal oxide electrode was extended to paraoxon detection. Paraoxon undergoes hydrolysis by organophosphorus hydrolase (OPH), an enzyme that is specific in its action towards OPs (Lai et al., 1994). The hydrolysis results in the generation of protons, which can be transduced into a measurable signal by the iridium oxide pH-sensing electrode.

3.4.1 Protein Immobilization

The technique for immobilizing the proteins on a glass slide was modified slightly from an earlier procedure developed using titanium oxide precoated glass slides(Ramanathan and Simonian, 2007). The exception from the earlier method involves the absence of step requiring fluorophore conjugation on protein immobilized slides. Briefly, the glass slide was cleaned by incubating it in 1N HCl for 30 minutes. It was, then rinsed thoroughly with DI water to remove any unwanted impurities and finally dried under nitrogen. The cleaned glass slide was held firmly by its sides on a rigid surface by 3M scotch adhesive tape. Titanium nanoxide paste that was obtained from Solaronix (Switzerland) was coated on the glass slide with the help of a glass rod using the "Doctor Blade squeegee printing method". This coated glass slide was placed in a furnace at 450°C for 30 minutes to enhance the adhesion of titanium oxide to slide. It was then cooled down to room temperature. Silanization of the titanium oxide coated slide

was done by placing it in 2% MPTS (3-mercapto propyl-trimethoxy silane) prepared in dry toluene for one hour. The glass slide was then rinsed in toluene and dried under nitrogen. This was followed by incubation in 1mM GMBS (N-γ-maleimidobutyryloxy succinimide ester) in prepared in ethanol for 45 minutes. The GMBS was first dissolved in DMSO (dimethyl sulfoxide) such that DMSO is 10% of the final volume. This process resulted in the thiother linkage between the maleimide group of GMBS and the sulfhydryl group of silane. After the cross-linking step, the slide was rinsed gently with DI water, dried under nitrogen and incubated in 1mg/ml of NeutrAvidin at 4°C in a refrigerator for 4 hours. After the NeutrAvidin step, the slide was rinsed in 10mM PBS buffer, pH 8.3. Biotinylation was done by incubating the glass slide in 1mg/ml biotin-XXSE for an hour. The biotin-XXSEE was prepared by first dissolving it in DMSO (10% of final volume) and then diluted in DI water. After the biotinylation step, the slide was rinsed with PBS buffer and dried under nitrogen. A physically isolated patterning block with polydimethyl siloxane (PDMS) similar to what was developed at the Naval Research Laboratories (NRL, Washington D.C) was developed in this work, to obtain a slide immobilized with spatially separated columns of proteins. Organophosphorus Hydrolase (OPH, 1 mg/ml) was immobilized on the slide by passing it through one of the channels by completely filling it. Similarly, Bovine Serum Albumin (BSA,1 mg/ml) a protein having a molecular weight similar to OPH without paraoxon hydrolyzing properties was passed on through another channel for its immobilization. Approximately, 150-175 μl of each protein solution was required to fill the channel. The entire set up was stored in a refrigerator at 4°C for 4 hours. At the end of 4 hours, the OPH and BSA solutions in the channels were removed and rinsed with PBS buffer. When the slide was not in use, it was

stored in the 10mM PBS buffer containing cobalt chloride at pH 8.3 under refrigerated conditions. **Figure 3.20** shows the patterning of the slide with OPH and BSA by various chemistries.
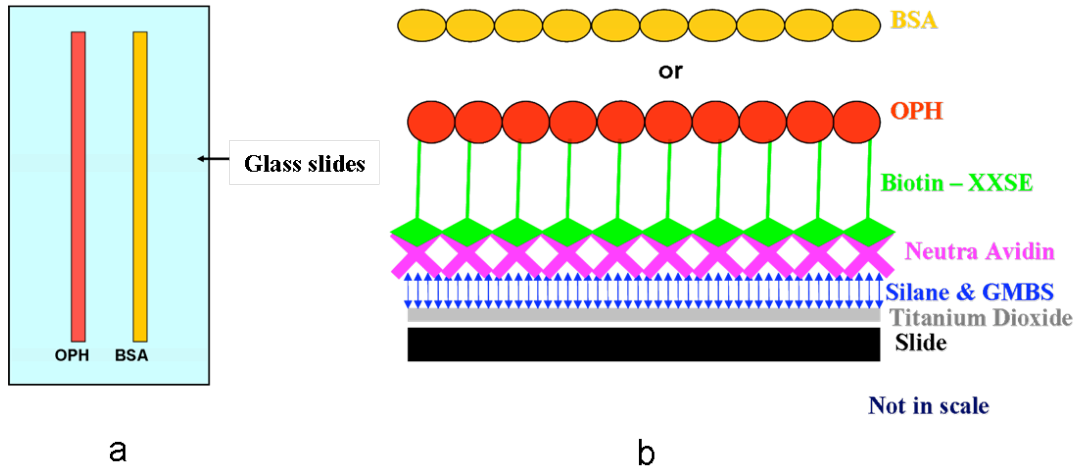
Figure 3.20: Immobilization chemistry and patterning of OPH and BSA on glass slide (a) Glass slide patterned with proteins (OPH and BSA), (b) Schematic of the chemistry used for protein immobilization

3.4.2 Multi channel pH sensor

The set up for multi-channel pH sensor consisted of the following parts: multi-channel PDMS flow block, iridium oxide coated titanium tubes, protein immobilized glass slide, plexiglas® slabs and PMD 1608 FS Data Acquisition (DAQ) device.

PDMS flow block was prepared using a design developed at the Naval Research Laboratories, Washington D.C. (Feldstein et al., 1999). In order to prepare the PDMS block, an aluminum mold containing six channels each of 40 x 2 x 2 mm was milled using a CNC milling machine at the welding laboratory of Materials Engineering

department, Auburn University. PDMS, mixed with an appropriate cross-linker (10:1 weight ratio) was degassed and cast onto the mold. This was allowed to cure at 80°C for 1 hour. The block was then allowed to cool down to room temperature and the hardened PDMS was carefully removed from the mold **(Figure 3.21a)**.

The electrode set-up was made by inserting a stainless steel tube at each end of two of the six channels in PDMS block to create inlets and outlets for solutions to pass through. Silicone tubes of an inner diameter of 1/8" were connected to the inlets and outlets of the stainless steel tubes. The silicone tubing at the outlet ends of the each channel were in turn connected to titanium tubes that were electrodeposited with iridium oxide films on their inner walls. This PDMS block with the channels was placed on the protein immobilized slide that was in turn held on a plexiglas®. Another plexiglas® was placed on the PDMS as shown in the **Figure 3.21b**. Screws were used to hold the plexiglas® with PDMS and glass slide to provide a good seal and prevent intermixing of solutions passing through BSA and OPH immobilized channels. The schematic of the multi-channel pH sensor is shown in the **Figure 3.22**

a   b
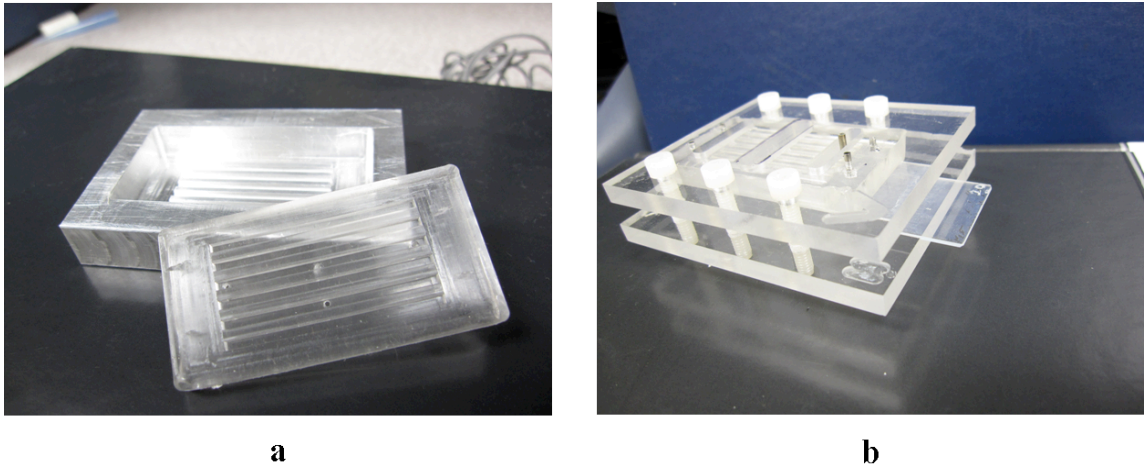
Figure 3.21: Multi-channel PDMS block for paraoxon detection (a) PDMS block from aluminum mold (b) Multi channel pH sensor
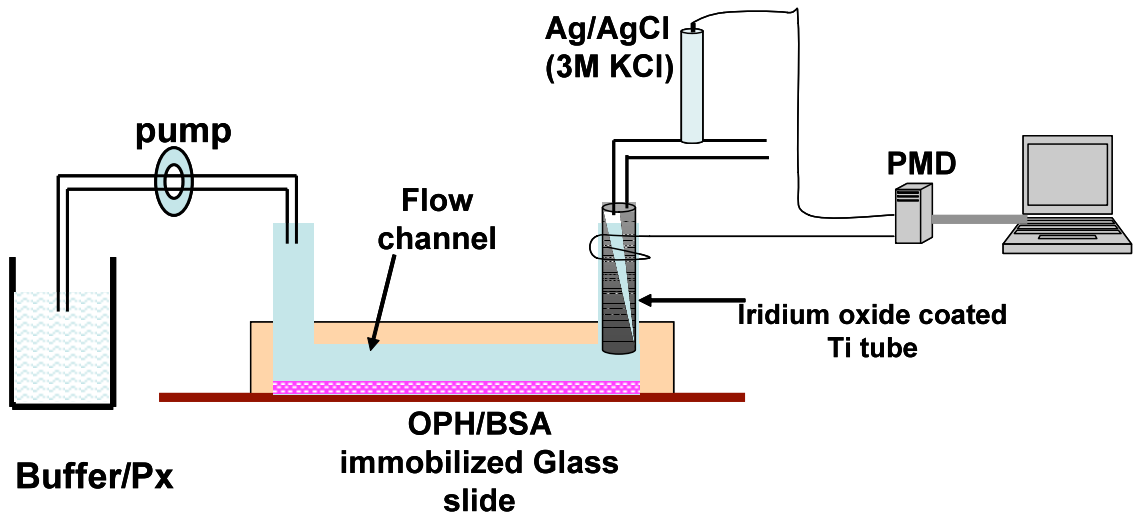
Figure 3.22: Schematic of the multi-channel pH sensor

The two titanium tubes connected to outlets of two channels were joined by a Y-connector to the flow through Ag/AgCl (3 M KCl) reference electrode **(Figure 3.23)**. The buffer or sample pumped to the two channels combined after passing through the pH sensitive iridium oxide coated titanium tubes before it entered the flow through reference electrode. This setting allowed the use of a single reference electrode for both the iridium oxide coated titanium tubes.

Figure 3.23: Flow through reference electrode

The Data Acquisition device PMD 1608 FS has 40 pins with 1-20 on one side and 21-40 on the other side. The pins 1 and 3 were used for measuring voltage and pin 2 was internally grounded (zero potential). The titanium tubes at the outlets of OPH and BSA channels were connected to pins 1 & 3 respectively by copper wires. The flow-through Ag/AgCl (3 M KCl) reference electrode was connected to pin 2. The potential difference between pins 1 and 2 were measured and termed as OCP of working (OPH) channel. Similarly, the potential difference between pins 3 and 2 measured the OCP of the reference (BSA) channel.

The PMD 1608 FS (DAQ) was connected to a computer through a USB port. Instacal® software (Measurement and Computing™) was used to acquire the potentials from pins on the DAQ device. The real-time data (potential vs time) was exported to Microsoft excel program.

3.4.3 Experimental procedure for paraoxon detection

Peristaltic pump was used to control the flow of buffer and paraoxon solutions. Initially, buffer (1mM PBS, 100µM $CoCl_2$) was allowed to flow through the protein immobilized channels. The buffer solutions were allowed to flow until the potentials were found to be stable and then the paraoxon solution was started to flow. When the paraoxon reached the two channels (OPH and BSA), the flow was stopped for 1 minute to allow the hydrolysis of paraoxon, and then the flow was resumed, allowing the solution in the channels to flow through the iridium oxide coated titanium tubes. These two streams of paraoxon were joined by the Y-connector before they reached the flow-through reference electrode. The process was repeated for different concentrations of paraoxon to obtain a response curve.

3.5 SEM studies

The surfaces of modified, un-modified glassy carbon electrodes and iridium oxide deposited titanium substrates were studied with a field emission Scanning Electron Microscope (SEM, JSM 7000F) by JEOL (Waterford, VA) equipped with an energy dispersive X-ray analyzer (EDX).

CHAPTER 4

RESULTS AND DISCUSSION

4.1 TCP detection

4.1.1 Electrochemical response of cresols

Cyclic voltammetry was performed to determine the electrochemical activity of cresols. A batch mode three-electrode cell was used in which glassy carbon, platinum wire and Ag/AgCl (3 M KCl) served as the working, auxiliary and reference electrodes respectively **(Figure 3.9).** The first cyclic voltammogram (CV) was taken in 5 ml of 10 mM PBS buffer, pH 7.4 between 100 mV and 900 mV *vs*. Ag/AgCl (3 M KCl) reference electrode at a scan rate of 50 mV/s. The electrode was then removed, polished and rinsed in DI water. O-cresol was added to the buffer solution such that the final concentration was 100 µM and a second CV was recorded.

Figure 4.1 shows the two cyclic voltammograms recorded with and without the addition of o-cresol. From the CVs, it can be seen that the addition of o-cresol produced a peak at around 0.6 V *vs*. Ag/AgCl (3 M KCl) in the forward scan. No peak was observed in the reverse scan. The absence of a reduction peak suggests that o-cresol undergoes irreversible oxidation at around 0.6V. **Figure 4.2** shows the linear sweep voltammetry for different concentrations of o-cresols (2 µM, 20 µM and 40 µM) at a scan rate of 50

mV/s in 10 mM PBS buffer, pH 7.4. The response current of an electro-active species which either undergoes oxidation or reduction is given by the difference in peak currents for the sample and buffer solutions respectively. As observed, all the cresol samples showed an oxidation peak around 0.6 V *vs.* Ag/AgCl (3 M KCl) and the peak currents (Δi_1, Δi_2 and Δi_3) increased with the increasing concentrations of cresols.
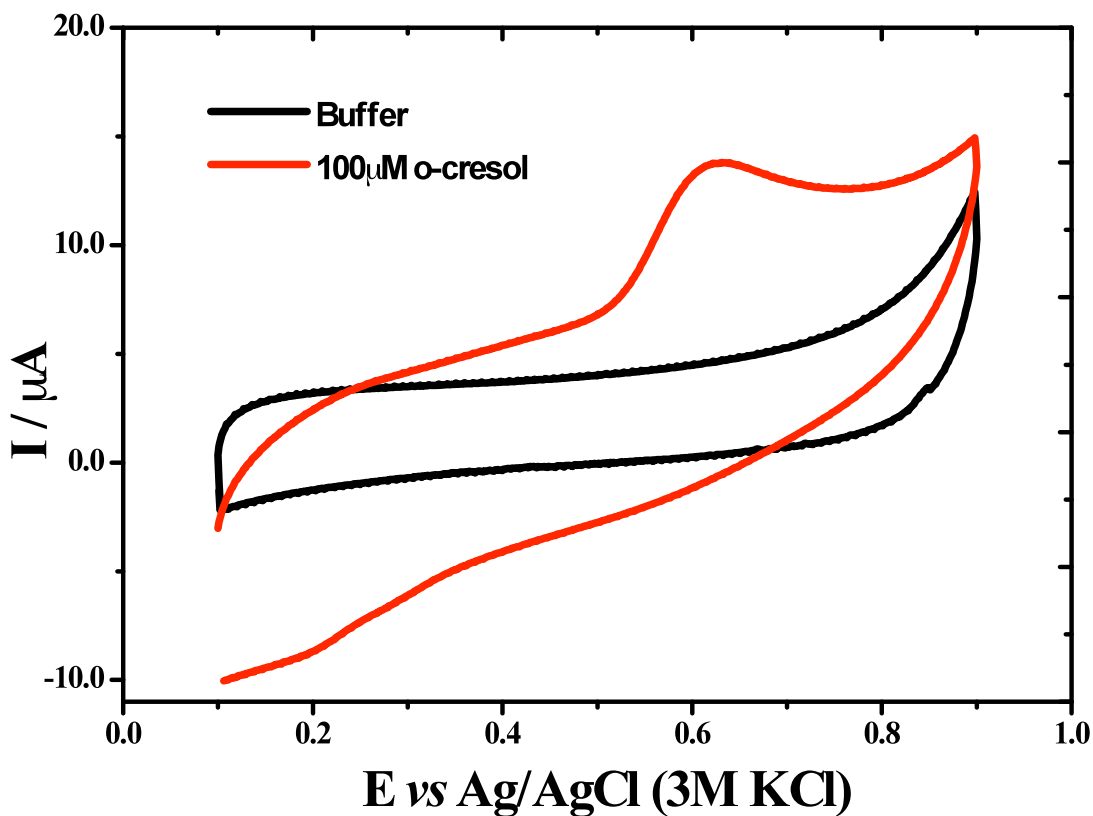
Figure 4.1: Cyclic voltammograms of 10mM PBS buffer, pH 7.4 and 100 μM o-cresol in 10 mM PBS buffer at pH 7.4 at a scan rate of 50 mV/s
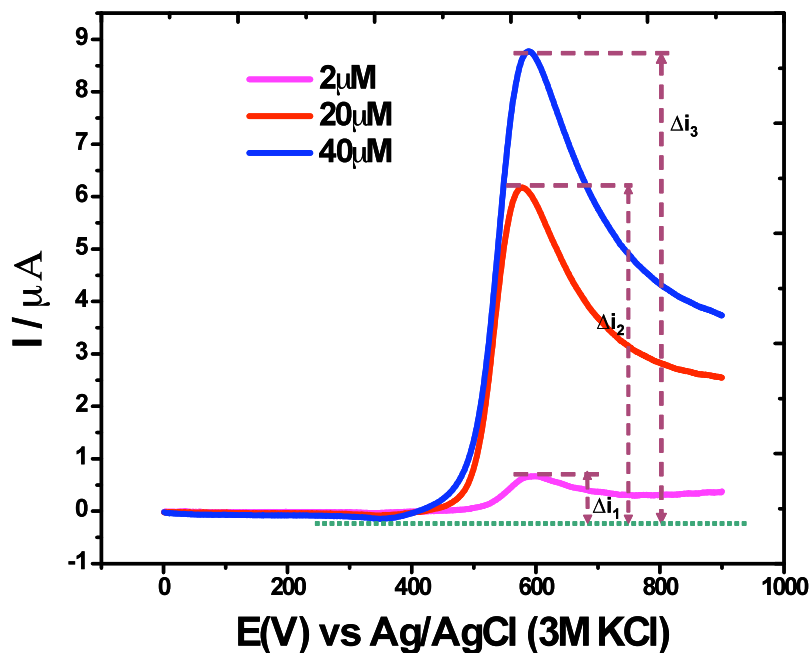
Figure 4.2: Linear sweep voltammograms for three concentrations of o-cresols namely, 2 μM, 20 μM and 40 μM at a scan rate of 50 mV/s (after background subtraction)

4.1.2 Glassy Carbon/Multiwalled-carbon nanotubes (GC/MWCNT) and glassy carbon/multi-walled carbon nanotubes modified with copper nanoparticles (GC/MWCNT-Cu)

Multiwalled-carbon nanotubes find increasing applications in the development of electrochemical sensors as they offer the advantages of providing high surface area for electron transfer, fast response times and high sensitivities(Qiang, Zhenhai et al., 2002).

71

In this study, the glassy carbon (GC) electrode was modified with multi-walled carbon nanotubes (GC/MWCNT) and copper nanoparticles (GC/MWCNT-Cu) were deposited on these nanotubes to enhance the response current.

4.1.2.1 Scanning electron microscopy (SEM) studies

SEM was used to study the copper nanoparticles that were electro-deposited on MWCNTs. **Figure 4.3** shows the distribution of copper nanoparticles on MWCNTs for different deposition times. The images show an increase in amount of Cu-nanoparticles with increasing deposition times. The presence of copper nanoparticles that are barely visible excepting the few shiny regions on MWCNTs attributed to its conductivity for 30 s deposition time becomes more prominent for 60 s deposition time. The size distribution of the particles from SEM was estimated to be around 50-70 nm. There is a further increase in the presence of copper nanoparticles for 120 s deposition time. In addition, 120 s deposition time shows relatively greater coalescence compared to 60 s. Also, other studies performed in our group on the electrochemical response of copper nanoparticles deposited on MWCNT for 120 s were unfavorable. The lower response for higher deposition time resulting in higher Cu-nanoparticle presence was in good agreement with studies in literature (Valentini, Biagiotti et al., 2007). Thus, 60 s was used to prepare GC/MWCNT-Cu electrodes for further studies. The presence of copper on the GC/MWCNTs was confirmed using EDX studies as shown in **(Figure 4.3 D)** for 60 s deposition time.
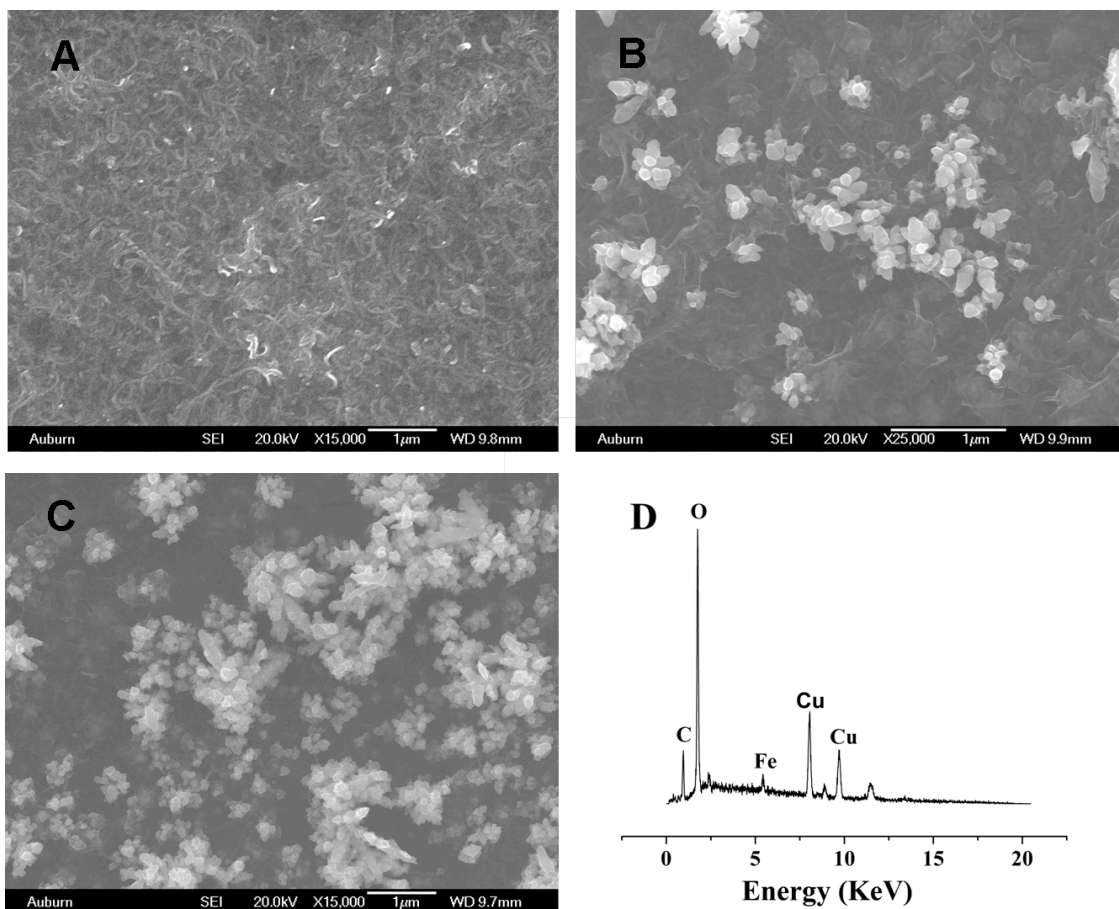
Figure 4.3: SEM image of copper deposited on GC/MWCNT electrode from 0.1M

Na_2SO_4 + 2 mM $CuSO_4$ at -1V vs Ag/AgCl (3 M KCl) for various deposition times.

A) 30 s B) 60 s C) 120 s D) EDX of GC/MWCNT-Cu for 60 s deposition time

4.1.2.2 Electrochemical response of GC/MWCNT and GC/MWCNT-Cu electrodes

Electrochemical response of the prepared electrodes were characterized by performing cyclic voltammograms (CVs) on bare glassy carbon (GC), GC/MWCNT and GC/MWCNT-Cu nanoparticle electrodes in 100 µM o-cresol in 10 mM PBS buffer, pH 7.4. These CVs were taken at a scan rate of 50 mV/s between 100 mV and 900 mV *vs.* Ag/AgCl (3 M KCl). The results from **Figure 4.4** show plain GC exhibits the oxidation voltage at ~ 0.6 V. The modification of GC electrode with MWCNTs reduced the oxidation potential to ~ 0.58 V. The introduction of copper metal nanoparticles further reduced the oxidation potential to ~ 0.55 V.
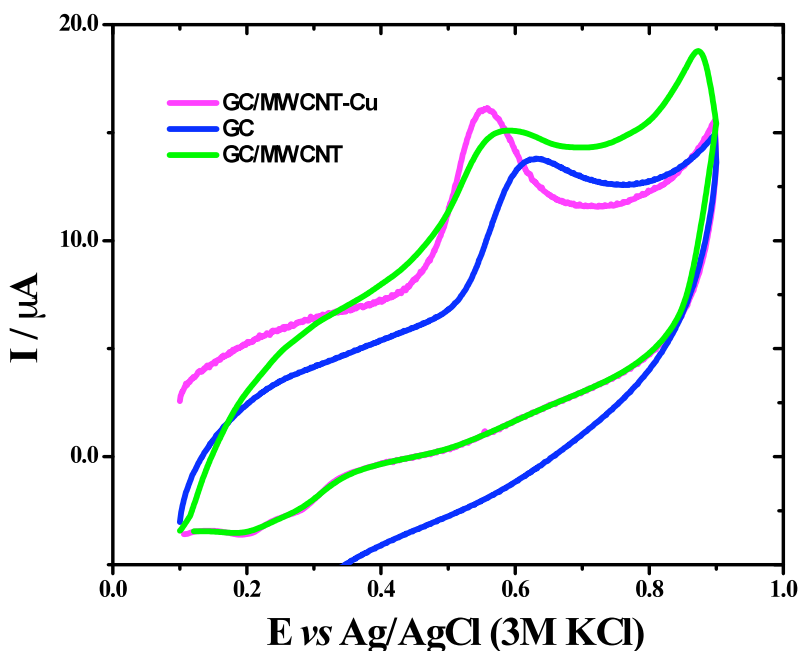
Figure 4.4: Cyclic voltammograms of 100 uM cresol on bare GC (blue curve), GC/MWCNT (green curve) and GC/MWCNT-Cu (pink curve) electrodes in 10 mM PBS buffer, pH 7.4

A similar increase in trend was observed for the peak currents GC, GC/MWCNT and GC/MWCNT-Cu electrodes respectively. This enhancement in electrochemical response is attributed to the synergistic electrocatalytic action of the GC/MWCNT-Cu composite.

4.1.3 Fouling of the working electrode

Oxidation of cresol at the surface of the working electrode results in the formation of a phenoxy radical which is highly reactive and exists in three different resonance structures as shown in **Figure 4.5**. This phenoxy radical reacts with another such radical (of different resonance structure) to form a dimeric polymer product as shown in **Figure 4.6.** This dimer is insoluble in the buffer solution and sticks onto the surface of the working electrode.
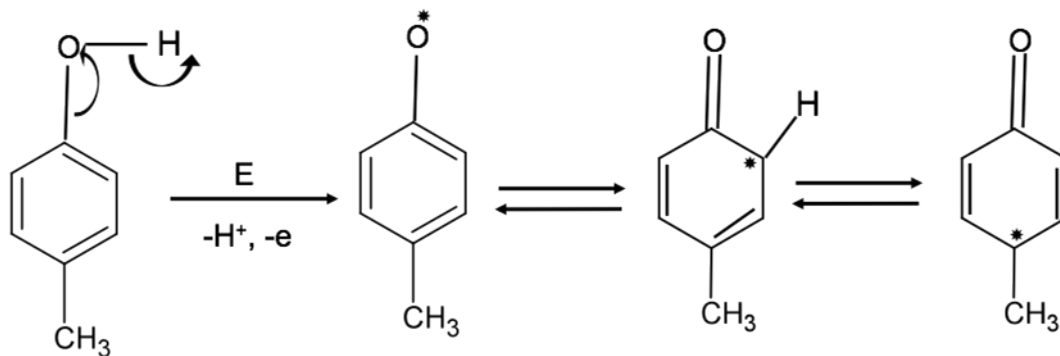
Figure 4.5: Formation of phenoxy radical and resonance structures upon oxidation of o-cresol
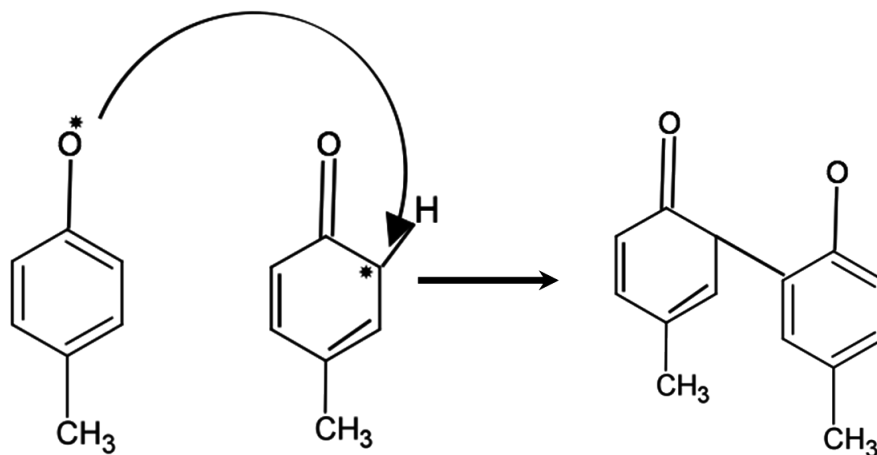
Figure 4.6: Formation of the dimeric polymer product formed by reaction between two phenoxy radicals

The dimeric polymer product was believed to act as a barrier for further oxidation of cresols. This was observed when 70μM of o-cresol were injected multiple times into a three electrode flow based electrochemical cell using the 12 port Valco™ injection system. The peak current was found to decrease with successive injections and a 27% decrease in peak current was observed at the end of 10th injection as shown in the **Figure 4.7.**
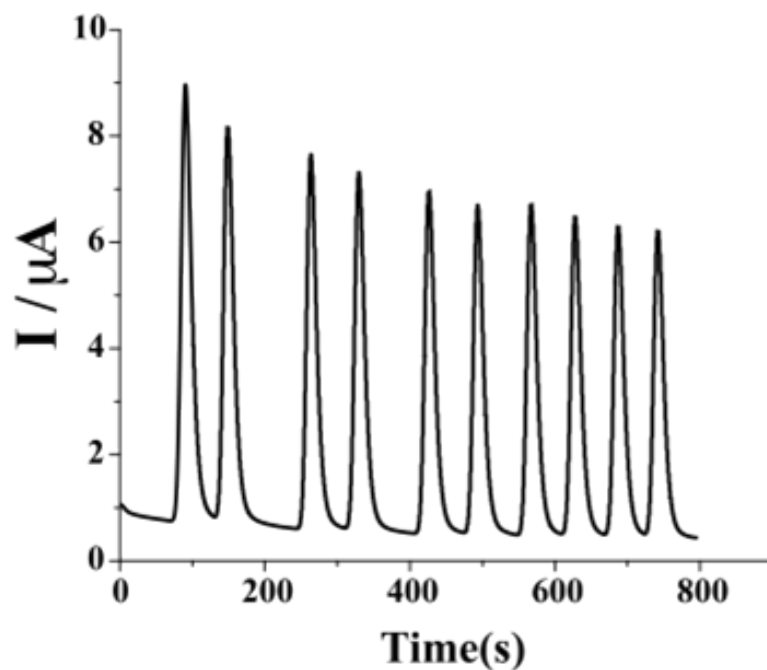
Figure 4.7 Flow injection Analysis (FIA) of 70 μM o-cresol in 10mM PBS buffer, pH 7.4 on the GC/MWCNT-Cu electrode under applied potential of 0.54V *vs*. Ag/AgCl (3 M KCl)

To address this problem, an anti-fouling agent, namely, Sodium 3,5 dibromo-4-nitroso benzene sulfonate (DBNBS) was used in this study. By using this compound, the phenoxy radical produced on cresol oxidation, reacts with DBNBS to form a non-adherent, buffer soluble compound (**Figure 4.8**). Hence, the DBNBS reagent scavenges the oxidized cresols and bypasses the reaction towards forming a harmless product, thus protecting the electrode.
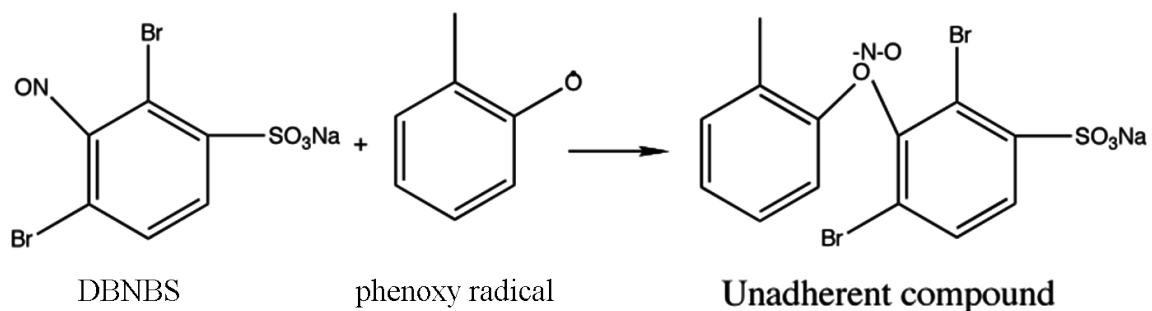
Figure 4.8: Formation of an unadherent, buffer soluble compound by reaction between phenoxy radical and DBNBS reagent

Figure 4.9 shows the flow based amperometric detection of 70 µM o-cresol in 10 mM PBS buffer, pH 7.4 when mixed with DBNBS reagent in the ratio of 1:1. Unlike the **Figure 4.7**, **Figure 4.9** exhibits no appreciable decrease in peak current at the end of 8th injection of cresol was observed. Hence, it was concluded that DBNBS was a capable anti-fouling agent in the current application by reacting with the oxidation product of cresol to form a non-adherent, buffer soluble compound.
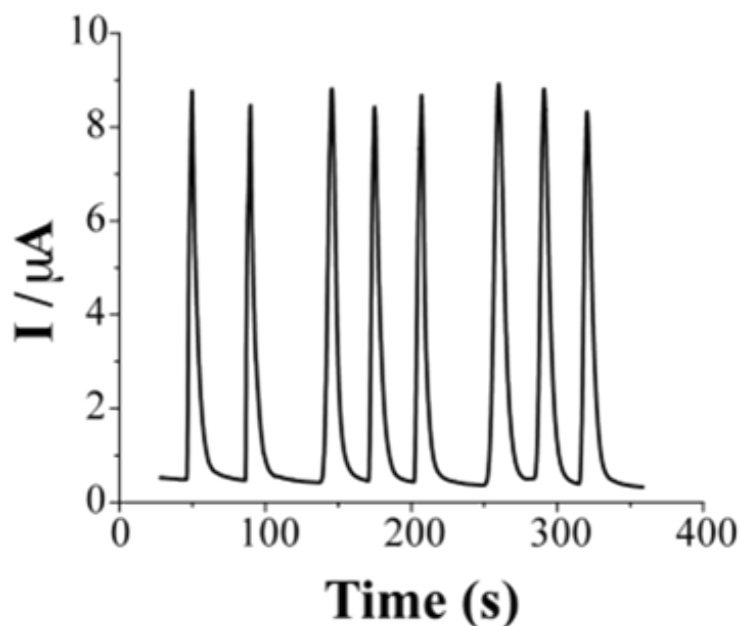
Figure 4.9: Flow injection Analysis (FIA) of 70 μM o-cresol in 10 mM PBS and 70 μM DBNBS in 10 mM PBS buffer, pH 7.4 on the GC/MWCNT-Cu electrode under an applied potential of 0.54V *vs*. Ag/AgCl (3 M KCl)

4.1.4: Sensitivity of the modified electrodes

Batch amperometric experiments were conducted on the prepared electrodes under stirring conditions to determine their response towards the oxidation of cresol. 0.5 V *vs*. Ag/AgCl (3 M KCl) was applied to GC/MWCNT-Cu nanoparticle electrode and 0.7 V *vs*. Ag/AgCl (3 M KCl) to GC/MWCNT and bare GC electrode respectively. After establishing a background non-faradaic current with 10 mM PBS, pH 7.4, o-cresol with DBNBS in 1:1 ratio was introduced to the stirring solution. An increase in current due to

cresol oxidation was observed in the form of step for all the three electrodes **(Figure 4.10)**. However, the amplitude of increase observed was different for every electrode, with GC/MWCNT-Cu showing the highest increase in current followed by GC/MWCNT electrodes. Unmodified-GC electrodes showed the least response in terms of change in current**.**
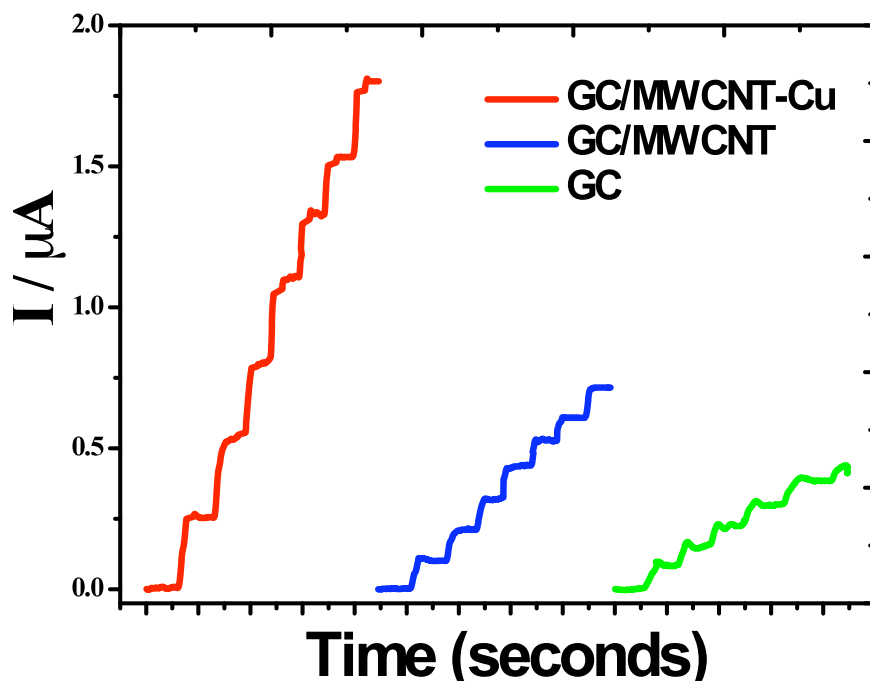
Figure 4.10: Batch amperometric measurements of cresol injections along with DBNBS for GC, GC/MWCNT and GC/MWCNT-Cu electrodes

Figure 4.11 shows the response curve in which the current values were plotted against various concentrations of cresol. The response was found to be linear in the given range of cresol concentrations that were tested. Slopes obtained from linear regression plots were used to determine the sensitivity of the electrode. Maximum slope and hence sensitivity, was obtained for GC/MWCNT-Cu electrodes. As discussed in the earlier

sections, this enhanced sensitivity can be attributed to the catalytic effect of the MWCNT-Cu composite.
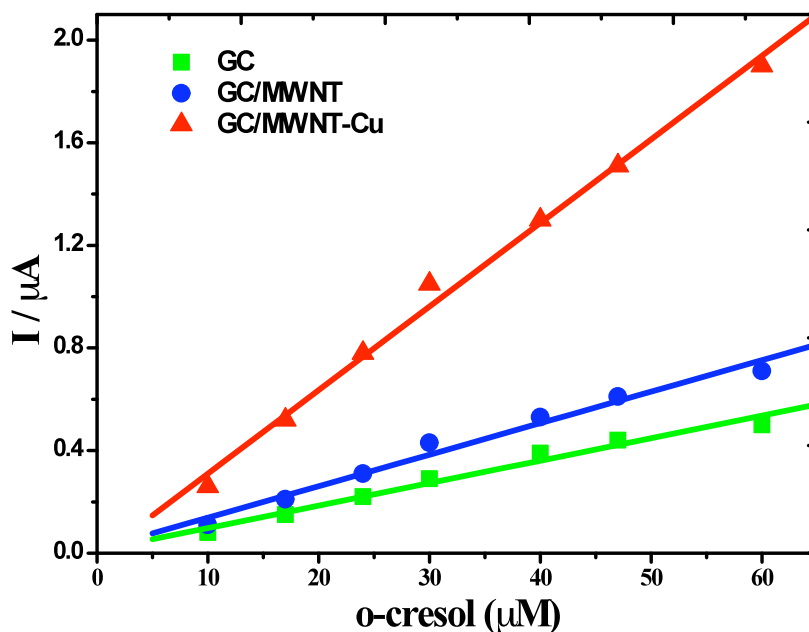
Figure 4.11: Response curve obtained for various concentrations of o-cresol using GC, GC/MWCNT and GC/MWCNT-Cu electrodes

The equations of the straight lines from the **Figure 4.12** are as follows:

$$GC: \qquad\qquad I = 0.01 + 0.01 \times [cresol], \quad r^2 = 0.989$$

$$: \qquad GC/MWCNT: \qquad I = 0.01 + 0.012 \times [cresol], \quad r^2 = 0.989$$

$$GC/MWCNT-Cu: \quad I = -0.15 + 0.032 \times [cresol], \quad r^2 = 0.998$$

4.1.5 Response in flow mode

The working electrode of the flow based three electrode cell was modified by casting multi-walled carbon nanotubes and electrodepositing copper nanoparticles on the nanotubes. Current response was observed for different concentrations of o-cresol with equimolar concentration of DBNBS reagent. **Figure 4.12** shows the response of the cresol (+DBNBS) solutions in 10 mM PBS buffer, pH 7.4. An increase in peak current was obtained with increase in cresol concentration with a sensitivity of 0.114 $\mu A/\mu M$ and a correlation coefficient of 0.957 **(Figure 4.13)**. A detection limit was found to be 0.6 μM based on the signal to noise ratio (S/N=3) characteristics.
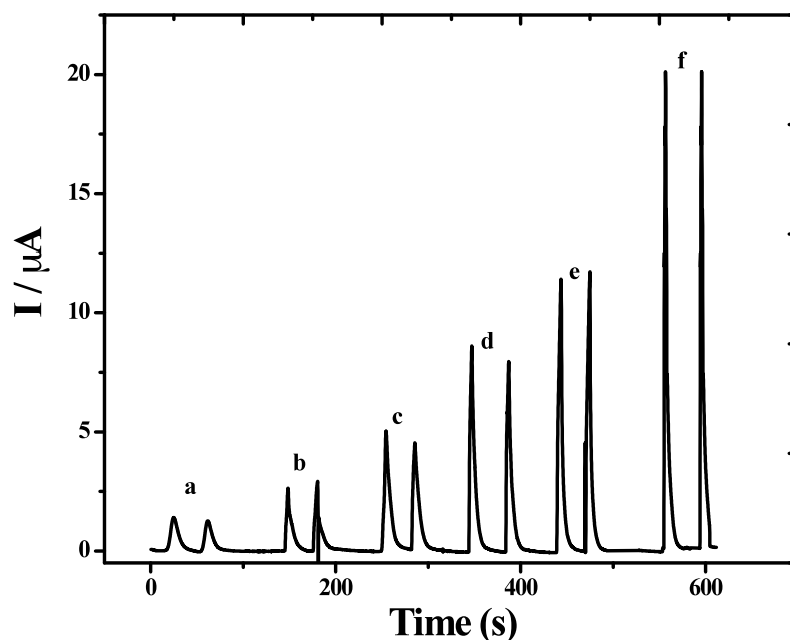
Figure 4.12: Flow injection analysis of 10 μM, 30 μM, 50 μM, 70 μM, 100 μM and 150 μM cresol with equimolar DBNBS reagent on GC/MWCNT-Cu electrode with an applied potential of 0.54 V *vs*. Ag/AgCl (3 M KCl)

82
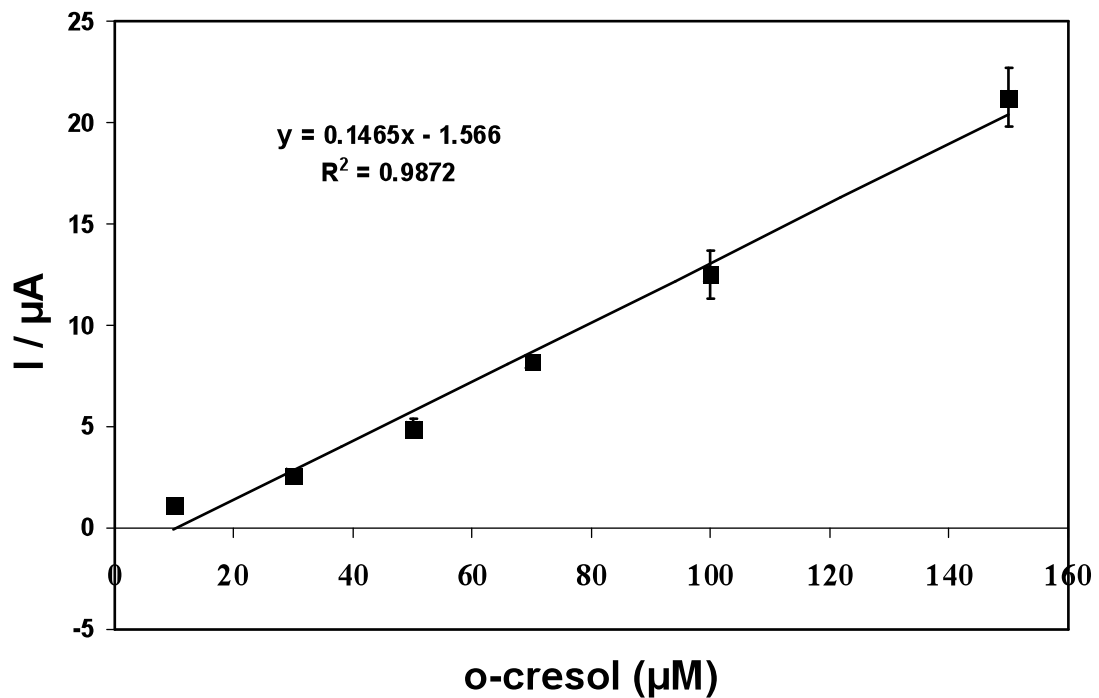
Figure 4.13: Response curve for different concentrations of o-cresol with equimolar concentration of DBNBS in flow mode with GC/MWCNT-Cu electrode in 10 mM PBS, pH 7.4 with an applied potential of 0.54V *vs*. Ag/AgCl (3 M KCl)

4.1.6 Effect of hydrolyzing media on TCP hydrolysis

Results discussed so far involved the use of cresols. Since the final target is tricresyl phosphates, it was essential to optimize the preparation of the hydrolyzing media contained in the column such that maximum conversion of TCP to cresols occurred, which could eventually be detected using the electrodes.

TCP was hydrolyzed in a media that was composed of different ratios of alumina (Al$_2$O$_3$) and sodium hydroxide (NaOH). In addition to the mixtures, individual influence of sodium hydrolixde and alumina was also studied in terms of TCP hydrolysis. In all the cases, TCP solution was directly treated with the hydrolyzing media. LSV was performed on the hydrolyzed TCP that produced cresols, at 50 mV/s between 100 mV and 900 mV *vs*. Ag/AgCl (3 M KCl) and their peak currents were compared to those obtained from known concentrations of cresols. The results obtained for various media prepared are tabulated in **Table 4.1.** The percentage conversion was calculated as follows:

$$\% \ conversion \ = \ \left(\frac{(Peak \ current)_{cresols} - (Peak \ current)_{hydrolyzedTCP}}{(Peak \ current)_{cresols}} \right) \times \ 100$$

It was observed that the percentage conversion for TCP to cresols was 100 % in the case of NaOH, while only 75-80 % hydrolysis of TCP was obtained when alumina was used. The percentage conversion of TCP to cresols increased with increase in the sodium hydroxide content in the NaOH+Al$_2$O$_3$ mixtures which was due to higher hydrolyzing ability of NaOH than Al$_2$O$_3$.

Although NaOH had better TCP hydrolyzing capability, it is a highly hygroscopic, corrosive and reactive chemical substance and is not safe for application in aircraft. Also, it produce leaks in the hydrolyzing column. Hence, its application for the development of a TCP hydrolyzing media for detection was not suitable. In this work,

Al$_2$O$_3$+10% NaOH was used for TCP hydrolysis as it could convert nearly 94-95% TCP into cresols and at the same time did not absorb much moisture and could be conveniently packed into the hydrolyzing column.

Hydrolyzing agent	% Conversion
NaOH (1M)	100
Al$_2$O$_3$	75-80
Al$_2$O$_3$+1%NaOH	80-85
Al$_2$O$_3$+2%NaOH	85-88
Al$_2$O$_3$+5%NaOH	88-94
Al$_2$O$_3$+10%NaOH	94-95
Al$_2$O$_3$+20%NaOH	95-96

Table 4.1: Effect of hydrolyzing media on the conversion rate of TCP to cresols measured by LSV in 10 mM PBS, pH 7.4

4.1.7 Detection of TCP from vaporized samples

Since the final objective of the study was to develop a sensor that is portable and easy to use for TCP detection in an aircraft, the sensors with the modified electrodes were integrated with a hydrolyzing column, an indigenously developed automated flow system and a wireless potentiostat.

Here, 10 ml of 20μM, 50μM and 100μM TCP samples were prepared in methanol solution and vaporized using an aquarium pump. After 5 minutes, the vaporized TCP was

adsorbed on to the modified alumina particles that formed the hydrolyzing column and the automated system Version 1.0 was initiated. 5 ml of 10 mM PBS buffer at pH 7.4 along with 500 µM of DBNBS was flushed through the hydrolyzing column. The obtained cresols were automatically injected into the flow based three electrode cell with MWCNT-Cu modified glassy carbon as the working electrode. The response current obtained upon oxidation of cresols at the working electrode was compared with the calibration curve for cresol detection in flow mode from **Figure 4.14.** According to the calibration curve, 18.5 µM, 45.5 µM and 92 µM concentrations corresponded to responses that were obtained for 20 µM, 50 µM and 100 µM concentrations of TCP respectively as indicated in **Table 4.2**.

Sample	*Add*	*Found*	*Recovery (%)*
A	20 µM	18.5 µM	92.5
B	50 µM	45.5 µM	91.0
C	100 µM	92.0 µM	92.0

Table 4.2: Recoveries of different concentrations of TCP in methanol

4.2 Determination of acid content in engine oils

4.2.1 Absorbance studies on the iridium oxalate deposition solution

Absorbance studies were made on the iridium oxide deposition solution during the course of its preparation at various steps using a UV-Vis spectrophotometer. **Figure 4.14** shows the changes in absorbance peaks and wavelength shifts that occur as the iridium oxide solution is prepared. An absorbance peak at 498 nm was observed when the

iridium (IV) chloride solution was dissolved in DI water. This absorbance peak was replaced by a small peak at 600 nm after the pH adjustment step which was attributed to the formation of iridium oxalate complex. The intensity of the 600 nm peak was found to increase as time elapsed from the day of sample preparation. As observed from the figure, the peak intensity at 600 nm plateaued after 6th day which suggests the completion of the complex formation.
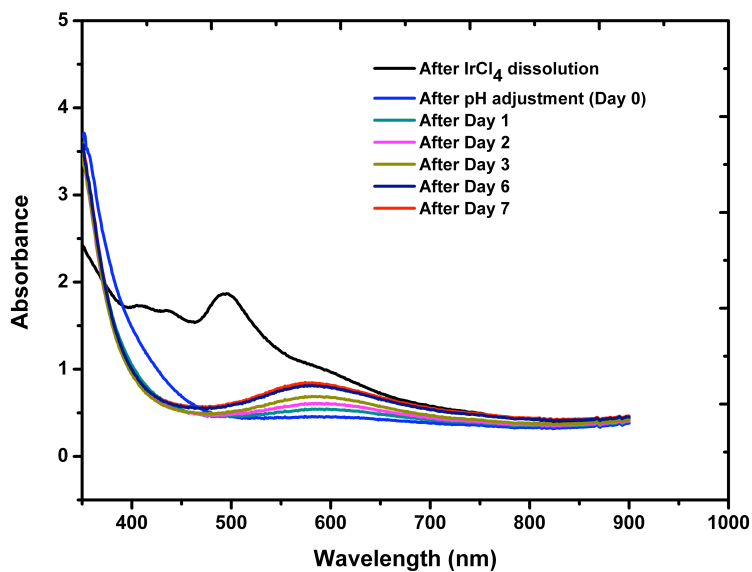
Figure 4.14. Absorption spectra of iridium chloride solution taken over a period of 7 days during the course of sample preparation

4.2.2 SEM studies of iridium oxide coated titanium substrate

Iridium oxide was coated on to a titanium foil substrate by galvanostatic method from the deposition solution at a current density of 2 mA/cm^2 for 180 seconds. After the electrode was rinsed in DI water and dried. **Figure 4.15** shows the SEM images of the iridium oxide films that were deposited on titanium foil at 3000X and 10000X

magnifications. The oxide films appeared to be porous and the particle size was estimated to be around 250nm.
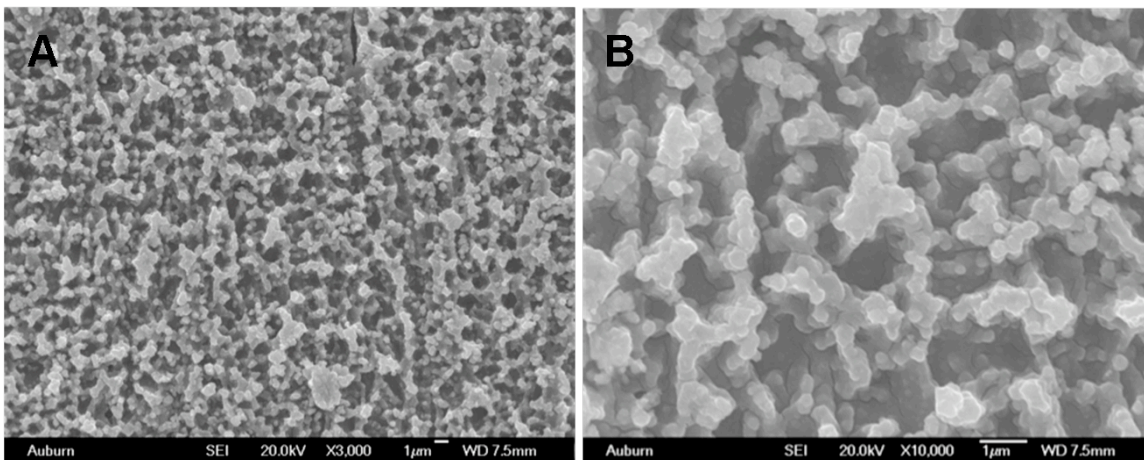
Fig 4.15. SEM image of at iridium oxide deposited on titanium foil by galvanostatic deposition of iridium oxalate solution under a current density of 2mA/cm^2 for 180 seconds. A) Magnification : 3000X B) Magnification: 10000X

4.2.3 Electrode response in buffers of different pH

Open Circuit Potentials (OCPs) were measured between iridium oxide coated titanium rod and Ag/AgCl (3M KCl) reference electrodes by a potentiostat from CH Instruments. Both the electrodes were dipped in a beaker containing at least 5 ml of buffer solutions adjusted to varying pH given in T**able 4.3**, using a pH glass electrode. The OCPs were measured for 5 minutes to allow the potentials to stabilize and the potential at the end of 5 minutes were used for calculating the pH sensitivity. **Figure 4.16** shows the OCPs measured in the buffers of different pH values. The electrode potentials

at the end of 5 minutes were calculated and plotted against the pH values as shown in the

Figure 4.17.
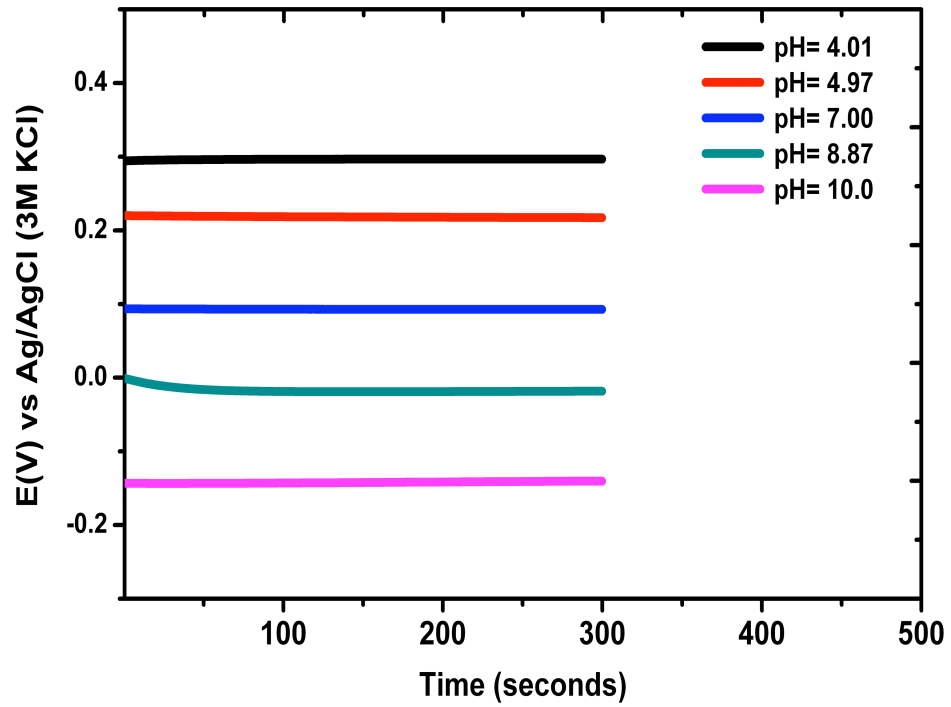
Figure 4.16. Open Circuit Potentials (OCPs) of iridium oxide coated titanium rod electrodes in buffers of varying pH
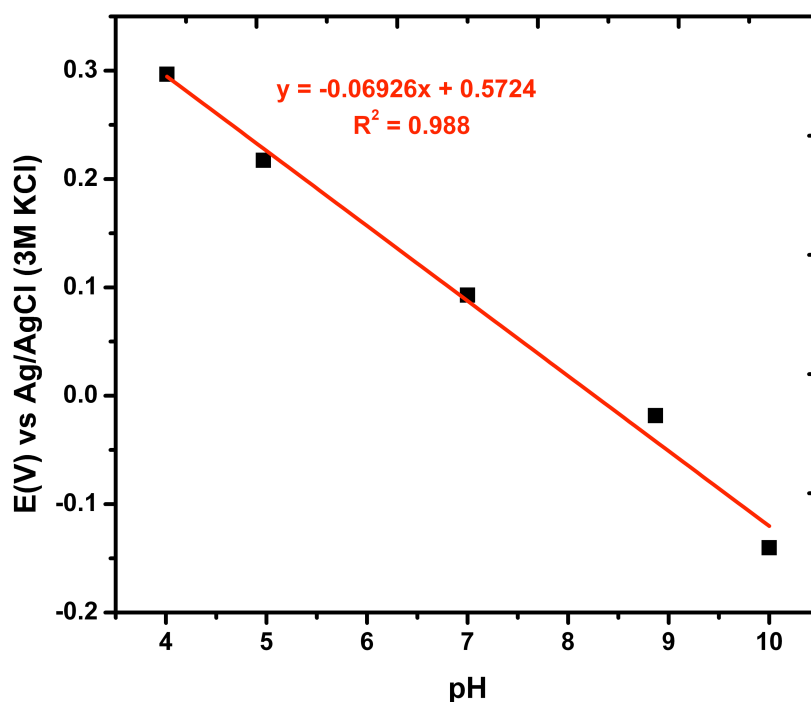
Figure 4.17. Electrode potentials at the end of 5 minutes of OCP measurement in buffers of varying pH

The pH sensing mechanism is based on the following redox reaction between hydroxylated Ir (IV) oxide and Ir (III) oxide.

$$2Ir(OH)_2O^- + H_2O \leftrightarrow IrO_2(OH)_3O_3^{3-} + 3H^+ + 2e^-$$

Since there are 3 hydrogen ions involved per 2 electrons in the above redox reaction in the Nernst equation, the pH sensitivity obtained should be 1.5 x 59 mV/pH, which is equal to 88.5 mV/pH. However, in the current study, pH sensitivities ranging

from 65 mV/pH to 80 mV/pH were obtained, which may be explained due to partial hydroxylation of the iridium oxide film (Pasztor et al., 1993).

Buffer	pH (measured from glass pH electrode)
50 mM potassium hydrogen phthalate	4.01
100 mM MES (2-(*N*-morpholino) ethanesulfonic acid)	4.97
50 mM sodium and potassium phosphate	7.00
50 mM CHES (2-[N-Cyclohexylamino] ethanesulfonic Acid)	8.87
25 mM sodium bicarbonate	10.00

Table 4.3. The table lists the buffers with different pH vales that were used for the OCP measurements

4.2.4 Stability studies

Two kinds of tests (Potential drift test and Sensitivity drift test) were conducted to determine the stability of the fabricated pH sensitive electrode. In the potential drift test, the OCPs were measured continuously for 5 hours to determine the drift in potential. **Figure 4.18** shows the stability of the electrode in terms of drift (mV/hr) in buffers at pH 4.07, 7.13 and 10.03. The OCPs approached their corresponding stable values by the end of 15 minutes and after an hour, the electrodes attained a drift of less than 10 mV/hr.

In the sensitivity drift test, the OCPs were measured continuously and their pH sensitivities were calculated over a period of 26 days. **Figure 4.19** shows the potentials recorded by the electrode in buffers of pH values 4.01, 4.97, 7.0, 8.87 and 10.0. From the

91

Figure 4.19, the OCPs were found to increase with time and became closer after day 11. Although, the OCPs were found to increase continuously with time, the sensitivities (calculated and given in **Table 4.4**) were relatively more stable and did not show any increasing trend.
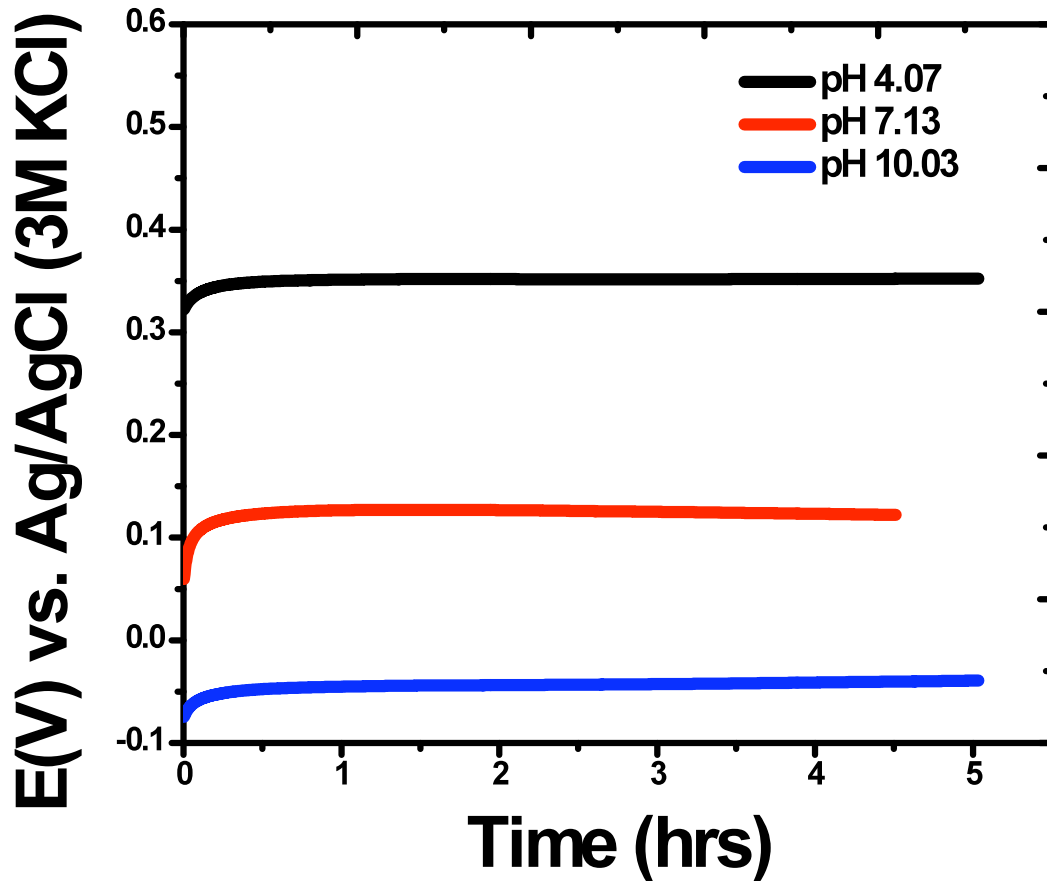

Figure 4.18. OCPs of the iridium oxide coated titanium rod electrode measured against Ag/AgCl (3M KCl) in buffers of pH 4.07, 7.13 and 10.03 for 5 hours
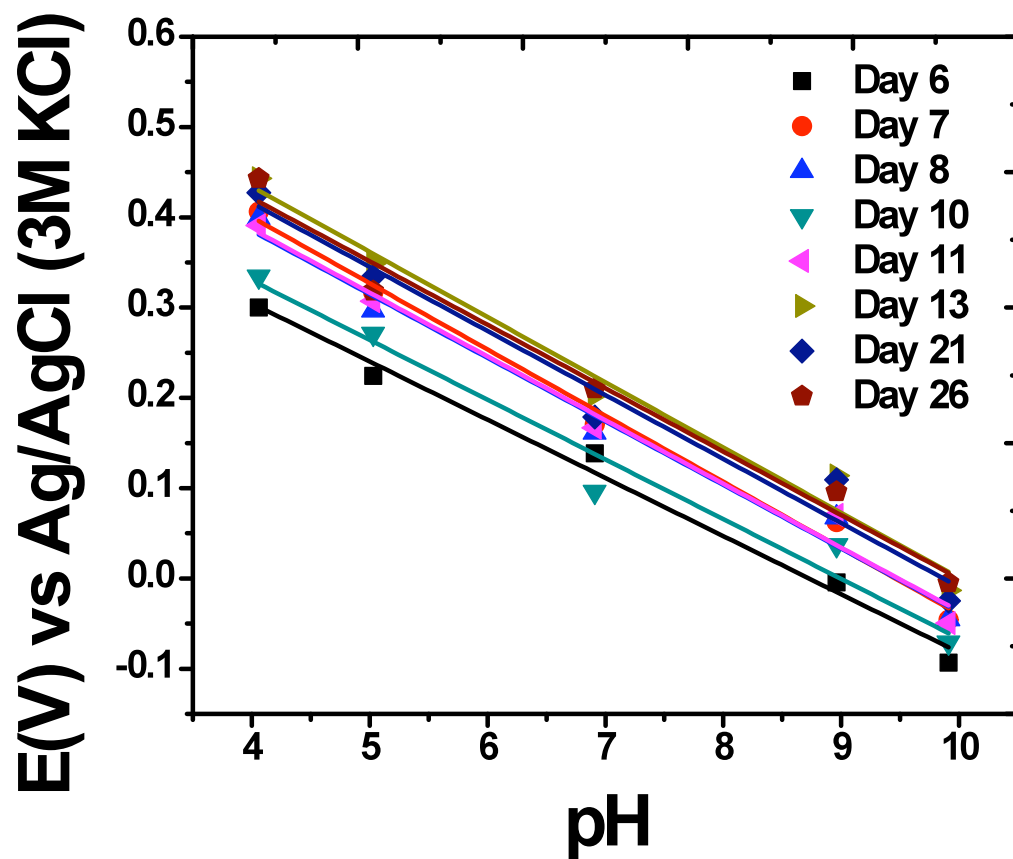
Figure 4.19. OCPs of the iridium oxide coated titanium rod measured against Ag/AgCl (3M KCl) in buffers of pH 4.01, 4.97, 7.0, 8.87 and 10.0 over a period of 26 days

Day	Sensitivity (mV/pH)
6	64.47
7	73.33
8	70.04
10	66.14
11	70.58
13	72.24
21	70.09
26	70.29

Table 4.4. Sensitivities of the iridium oxide coated titanium rod electrode measured against Ag/AgCl (3M KCl) in buffers of pH 4.01, 4.97, 7.0, 8.87 and 10.0 over a period of 26 days.

4.2.5 TAN and OCP measurement in artificially aged oils

British Petroleum Turbo Oil, BPTO 2380 was obtained commercially from an engine oil store. This oil was artificially aged at the Materials Engineering department at Auburn University by placing it in a heating chamber at 155°C. Samples of oil were procured after 12, 24, 48 and 96 hours of aging and the TAN of these oils was measured using *Koehler Instrument*'s Automatic Potentiometric Titrator (APT). This titration was based on ASTM D664 method in which the oil sample was continuously titrated with 0.1 N KOH and the potential of a glass pH electrode that was dipped inside the titration beaker was continuously recorded. The end point of titration was determined by the inflection point in the graph of potential versus volume of KOH used for titration. In this method, TAN was measured by the following formula:

$$TAN = \frac{EP \times C \times MW}{S} \, mg/g$$

Where,

EP = volume of KOH consumed till end point (ml)

C = Concentration of KOH (0.1N)

MW = Molecular weight of KOH (56.1)

S = Sample volume (g)

These calculations are done automatically by the Automatic Potentiometric Titrator (APT) and the final TAN results were displayed on the LCD panel and as a printout through the Impact dot printer.

TAN was measured by the APT on the fresh BPTO 2380 and the aged oils (12, 24, 48 & 96 hrs at 155°C) whose values are shown in **Figure 4.20**. The TAN values were found to increase with increase in the aging time, which suggests that increase in aging time results in the accumulation of acid content in the oils. This acid accumulation was due to the formation of carboxylic acids due to incomplete combustion of oils at elevated temperatures.

OCPs of fresh and artificially aged oils were measured by the pH sensitive iridium oxide rod electrode against Ag/AgO reference electrode. The oils samples were dissolved in a 1:10 ratio of oil to isopropanol and these dissolved oils were used for OCP measurement. The OCPs at the end of 5 minutes of measurement were recorded and plotted against the oil aging time. **Figure 4.21** shows that the OCPs of the pH sensitive

iridium oxide electrode increased with increase in the aging time. This indicates that the pH of the oils obtained after longer aging times were lower than no or shorter aging times. The decrease in the pH of the oils was due to the increase in hydrogen ion concentration and can be attributed to the acid formation on aging of the oil at high temperatures.
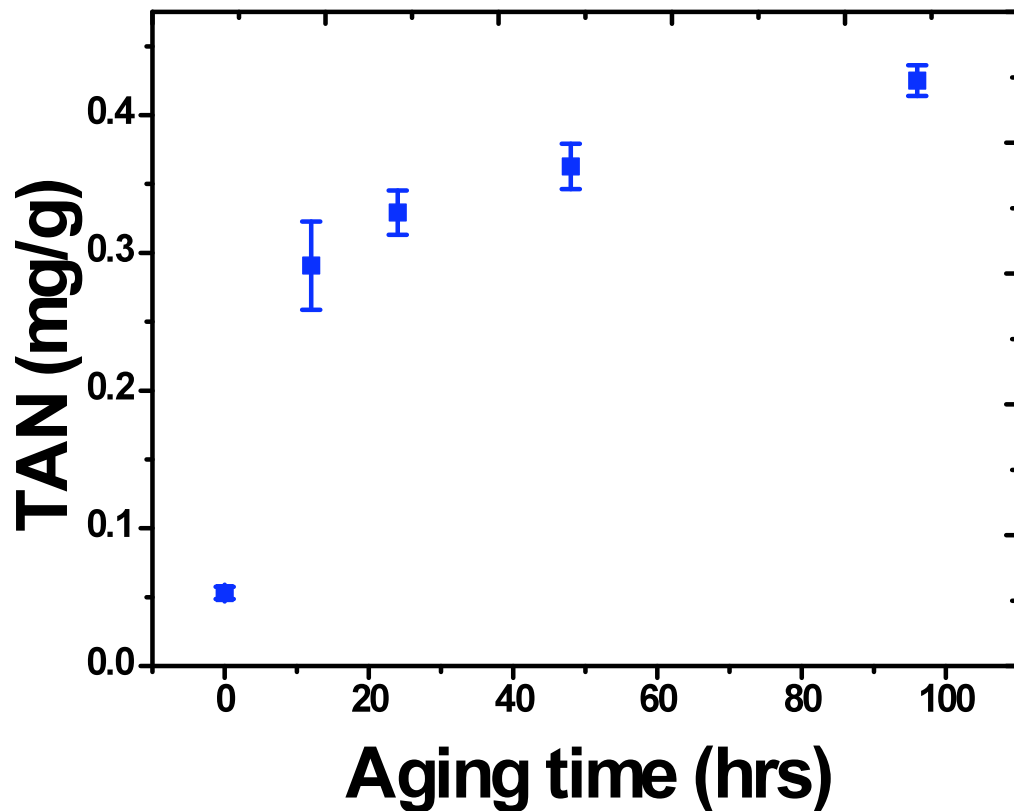
Figure 4.20. TAN measured from the Automatic Potentiometric Titrator by Koehler's Instruments on fresh and artificially aged BPTO 2380 oil at 12, 24, 48 and 96 hours at 155°C
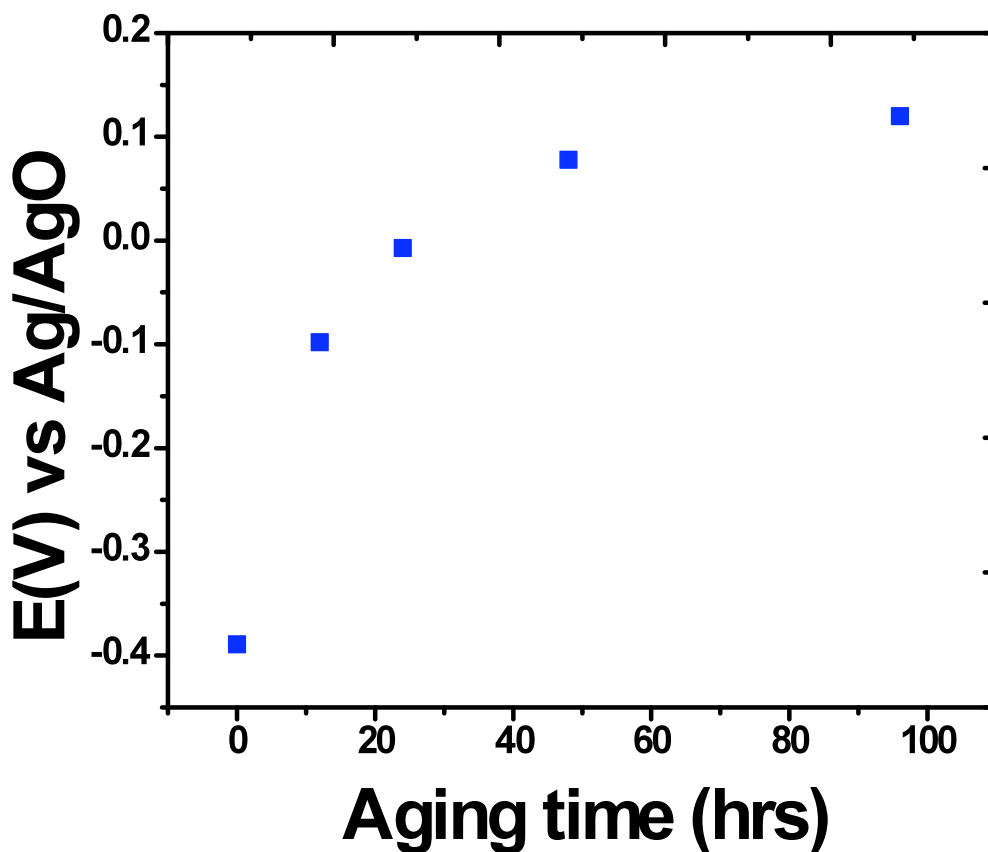
Figure 4.21. OCP measurement by the pH sensitive iridium oxide rod electrode in fresh and artificially aged BPTO 2380 oil at 12, 24, 48 and 96 hours at 155°C

4.2.6 Detection of OP neurotoxins – an extended application of pH sensing

Paraoxon, a toxic organophosphorus compound undergoes catalytic hydrolysis in the presence of an enzyme Organophosphorus Hydrolase (OPH) giving diethyl phosphate, para-nitrophenol and two protons, was choose as a modeling analyte. The production of protons decreases the pH of the solution which can be detected by pH sensitive iridium oxide electrodes.

4.2.6.1 pH response from OPH and BSA channels

Several electrodes were prepared by electrodeposition of iridium oxide on the inside walls of titanium tubes. Two electrodes were selected from the lot whose pH sensitivities are close to each other. These electrodes were connected to the outlets of the PDMS block. OPH and BSA patterned glass slide was embedded between the PDMS block and the plexi glass slabs. Buffers of pH 4.00, 7.00 and 10.00 were passed through both the channels and their OCPs were measured continuously. As shown in **Figure 4.22,** both the working electrodes showed a good correlation in their response to different pH values and their sensitivity was found to be 69mV/pH. . In order to get a response to various concentrations of paraoxon, 1mM PBS buffer adjusted to pH 8.3 was passed initially to get a background signal in both the channels. A low strength buffer was chosen to provide least resistance to changes in pH to in turn enhance sensitivity In **Figure 4.23**, the red and black curves represent the OCPs of the iridium oxide coated titanium tube electrodes of the solution (paraoxon/buffer) coming from OPH and BSA channels respectively.

The blue curve in **Figure 4.22** is the difference between the control (BSA) channel from the working (OPH) channel. The OCPs of the electrode from the OPH channel showed greater changes to paraoxon concentrations than the electrode from the BSA channel. This can be attributed to the enzymatic hydrolysis of paraoxon by OPH resulting in the release of hydrogen ions while in the case of BSA that does not have OP hydrolyzing properties, the changes in OCP are used to account for sample and buffer variations in pH.
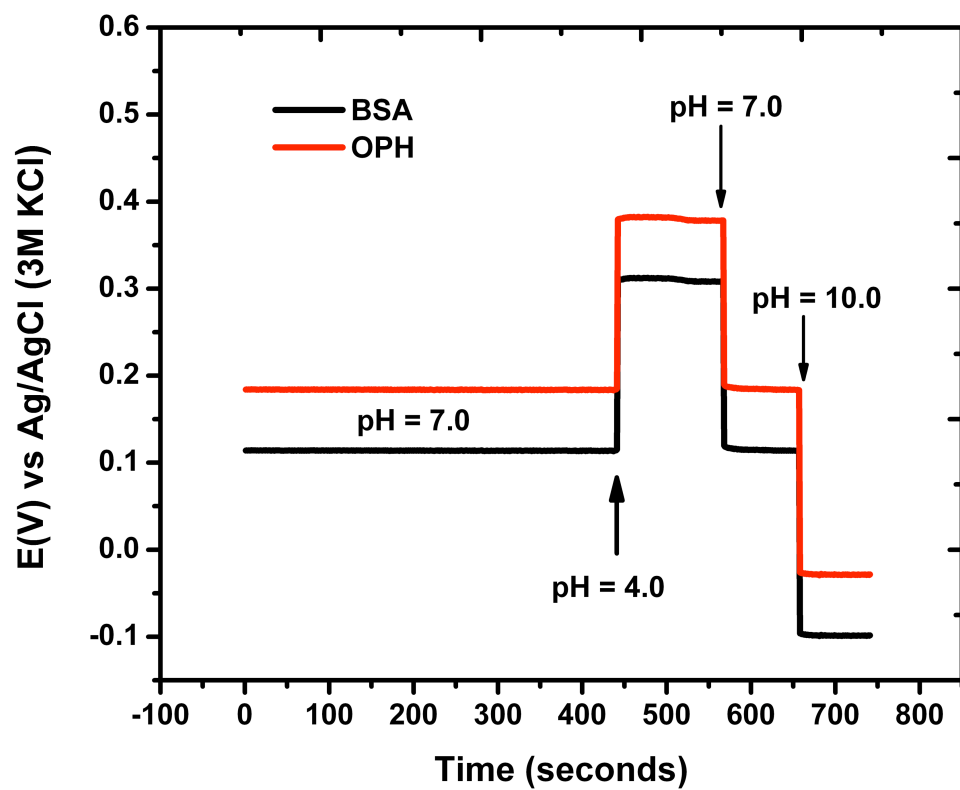
Figure 4.22 Electrode responses to pH 4.00, 7.00 and 10.00 from channels containing OPH and BSA
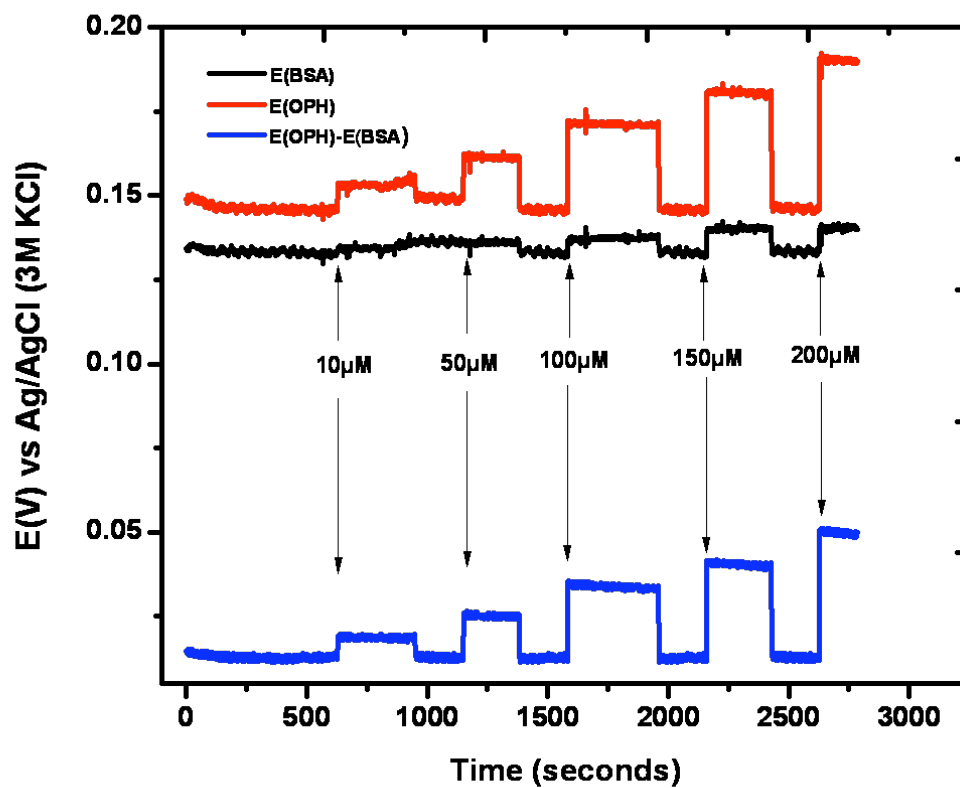
Figure 4.23. OCPs of iridium oxide coated titanium tube electrodes in 1mM PBS buffer, pH 8.3 and paraoxon concentrations 10 μM, 50 μM, 100 μM, 150 μM and 200 μM

4.2.6.2 Response curve

The change in the OCPs with the introduction of different concentrations of paraoxon was plotted as shown in **Figure 4.24**. A linear fit with a correlation coefficient of 0.9963 was obtained. The sensitivity calculated from the slope was found to be

0.1418mV/μM of paraoxon. A detection limit of 10μM was found for paraoxon as the

potential changes due to paraoxon concentrations below 10μM were less than the

acceptable signal to noise ratio (S/N=3).
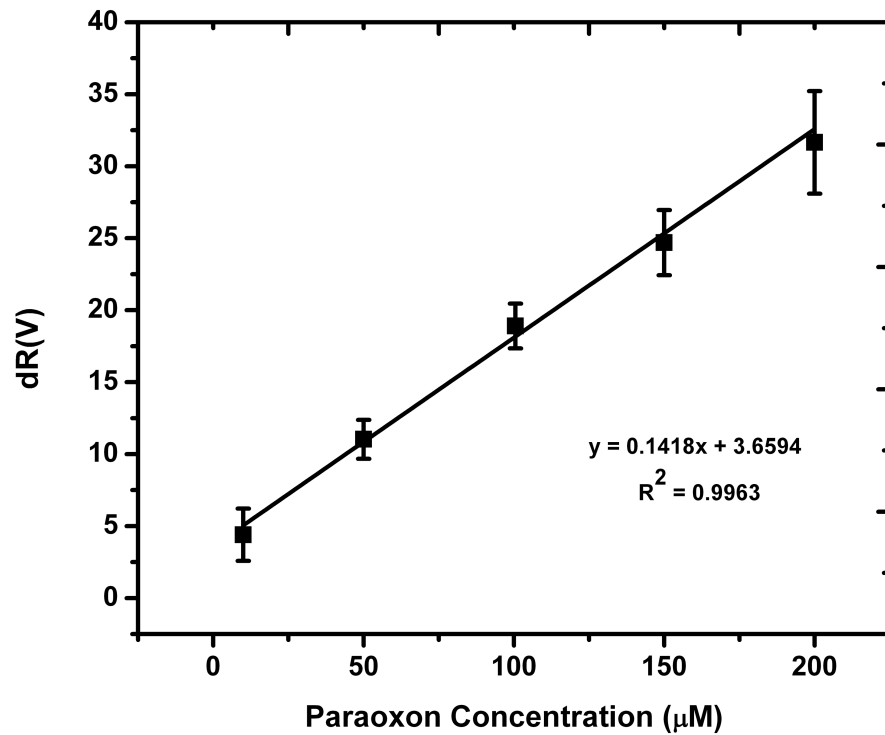
Figure 4.24. Response curve showing a linear region for paraoxon concentrations 10

μM, 50 μM, 100 μM, 150 μM and 200 μM in 1mM PBS buffer

CHAPTER 5

CONCLUSIONS AND FUTURE WORK

5.1 Conclusions

An automated electrochemical sensor was developed for the detection of tricresyl phosphate in air. A hydrolyzing column made of modified alumina was developed for the conversion of TCP to electro-active cresols that were detected electrochemically at the surface of glassy carbon electrode modified with multi-walled nanotubes and copper nanoparticles. The electrode modification decreased the oxidation potential of o-cresol from 0.6 to 0.54 V *vs.* Ag/AgCl (3 M KCl) and a three fold increase in sensitivity was obtained. An antifouling agent, Sodium 3, 5 dibromo-4-nitroso benzene sulfonate (DBNBS) was used to prevent the fouling caused by the formation of dimeric polymer film formed upon the electrochemical oxidation of cresols. A detection limit of 0.6 μM and a sensitivity of 0.114 μA/μM were obtained in flow mode for cresols using the modified glassy carbon electrode and in the presence of the anti-fouling agent, DBNBS. An automated system was developed in LabVIEW® to integrate the hydrolyzing column and the electrochemical sensor for easy operation for the aircraft crew.

Metal oxide pH sensors were developed for the detection of acid content in oil. Here, Iridium oxide films were deposited by anodic electrodeposition on titanium substrates such as foil, rods and tubes. SEM was done on the titanium foil electrode which revealed the presence of porous iridium oxide films. The pH sensitivities were calculated by measuring the OCPs in buffers of different pH. Sensitivity studies related to long term drift and long term sensitivity were performed. The electrode showed a drift of less than 10mV/hr after 5 hours and stable sensitivity of 70mV/pH by the end of 26 days. Total Acid Number (TAN) was measured using Automatic Potentiometric Titrator on artificially aged BPTO 2380 oils and OCPs of the oils samples were measured by the iridium oxide rod electrodes. The trend of TAN values of the artificially aged oils was consistent with the OCPs measured by the iridium oxide rod electrodes against a modified Ag/AgO reference electrode.

The pH sensing properties of iridium oxide were exploited for the detection of paraoxon using a multi-channel PDMS block. OPH and BSA were immobilized on the glass slide exposed to the flow channels in the PDMS block. Paraoxon which was introduced through both the channels, hydrolyzed only in the channel where OPH was immobilized generating protons which were detected by the pH sensing iridium oxide tube electrodes. A detection limit of 10 μM for paraoxon was obtained considering the signal to noise ratio characteristics.

5.2 Future work

Inspiring from the available electrochemical gas sensors, the sensor can be further miniaturized by micro-fabrication to a size of a penny by developing a three electrode

cell in which a solid electrolyte can be used which acts both as an electron transfer and TCP hydrolyzing medium.

The OCPs measured by the pH sensitive iridium oxide electrodes are made in diluted oil which prevents it from using directly in automobiles. The problem of high resistance of oil can be overcome by micro-fabricated inter-digitated electrodes (IDEs) such that the sensor can be directly embedded inside the engine oil tank and enabling continuous monitoring of acid content.

In the multi-channel PDMS block, the unused channels can be used for immobilization other enzyme to study the effect of their hydrolyzing abilities. Also, simultaneous detection of other organophosphorus compounds such as parathion, demeton-s, sarin, soman, etc., can be done using the multi-channel sensor.

REFERENCES

(1990). WHO ICPS: Tricresyl Phosphates, Environmental Health Criteria, WHO International Program on Chemical Safety. Geneca.

(1997). "James Lamb IV, Tricresyl Phosphate." Environmental Health Perspectives Supplements **105**(S1).

(2007). "ASHRAE Standard: Air Quality within Commercial Aircraft." American Society of Heating, Refrigerating and Air-Conditioning Engineers.

(2007). "Material Safety Data Sheet: Tricresyl Phosphates." Mallinckrodt Baker Inc. Retrieved June 2009, 2009, from http://www.jtbaker.com/msds/englishhtml/t5161.htm.

(2009). "Polaris Laboratories LLC: Base number." 2009, from http://www.polarislabs1.com/test-explanations/base-number.htm.

Abou-Donia, M. B. and Lapadula, D. M. (1990). "Mechanisms of Organophosphorus Ester-Induced Delayed Neurotoxicity: Type I and Type II." Annual Review of Pharmacology and Toxicology **30**(1): 405-440.

AFL-CIO (2003). Aircraft air quality: What's wrong with it and what needs to be done. Association, of, Flight and Attendents. Washington D. C., The Aviation Subcommittee of The Transportation & Infrastructure Committee U.S. House of Representatives**:** 1-40.

Aldridge, W. N. (1953). "Tricresyl phosphates and acetylcholinesterase." The journal of Biochemistry **56**: 185-189.

Andrews, G. E., et al. (2001). Oil quality with oil age in an IDI diesel passenger car using an online lubricating oil recycler under real world driving, Society of Automotive Engineers Inc.

Angel, W. (2008). "ASHRAE Publishes Nation's First Airplane Cabin Air Quality Standard."   Retrieved December 2008, 2009, from http://www.ashrae.org/pressroom/detail/16755.

Ardizzone, S., et al. (1981). "Properties of thermally prepared iridium dioxide electrodes." Journal of Electroanalytical Chemistry **126**(1-3): 287.

Barry, R. C., et al. (2008). "Nanotechnology-based electrochemical sensors for biomonitoring chemical exposures." J Expos Sci Environ Epidemiol **19**(1): 1.

Basu, A., et al. (2000). ""Smart Sensing" of Oil Degradation and Oil Level Measurements in Gasoline Engines." SAE transactions **109**(4): 857-863.

Belski, V. E. (1977). "Kinetics of the hydrolysis of phosphate esters." Russian Chemical Reviews **46**(9): 828-841.

Burke, L. D., et al. (1984). "Preparation of an oxidized iridium electrode and the variation of its potential with pH." Journal of Electroanalytical Chemistry **163**(1-2): 117.

Chambers, H. W. (1992). Organophosphorus compounds: An Overview. San Diego, Academic Press, Inc.

Chambon, L., et al. (1999). "A metallic oxide gas sensor array for a selective detection of the CO and NH3 gases." Sensors and Actuators B: Chemical **60**(2-3): 138.

Cheng, K. L. (1998). "Explanation of Misleading Nernst Slope by Boltzmann Equation." Microchemical Journal **59**(3): 457.

Cheng, K. L. (2002). "Recent development of non-faradaic potentiometry."
Microchemical Journal **72**(3): 269.

Collins, E. (1945). "Reaction of diazotised p-nitraniline with phenols: detection of
tricresyl phosphate in edible oil." The Analyst **70**: 326-330.

Cottington, R. L. and Ravner, H. (1968). Neopentyl Polyol esters for jet engine lubricants
effect of tricresyl phosphate on thermal stability and corrosivity. Washington D.C, Naval
Research Laboratories**:** 1-21.

Coverdell, A. (2007). "A Comprehensive Look At the Acid Number Test." Practicing Oil
Analysis Magazine(200707).

Craig, P. H. and Barth, M. L. (1999). "Evaluation of the hazards of industrial exposure to
tricresyl phosphate:a review and interpretation of the literature." Journal of Toxicology
and Environmental Health, Part B **2**(4): 281-200.

Currie, J. F., et al. (1999). "Micromachined thin film solid state electrochemical CO_2,
NO_2 and SO_2 gas sensors." Sensors and Actuators B: Chemical **59**(2-3): 235.

De Nola, G., et al. (2008). "Determination of ortho-cresyl phosphate isomers of tricresyl phosphate used in aircraft turbine engine oils by gas chromatography and mass spectrometry." Journal of Chromatography A **1200**(2): 211.

Dunlop, J. (2007). "Major Study of Aircraft Cabin Air Quality Launched." Retrieved May 2009, 2009, from http://www.ashrae.org/pressroom/detail/16102.

Eilhard, J. (1996). "The origins of synthetic lubricants: The work of Hermann Zorn in Germany part 1 basic studies of lubricants and the polymerisation of olefins." Journal of Synthetic Lubrication **12**(4): 283-301.

Elliott, W. N., et al. (1972). "Determination of phosphorus in lubricating oils by cool-flame emission spectroscopy." Talanta **19**(3): 359.

Eyer, P. (1995). "Neuropsychopathological changes by organophosphorus compounds -- a review." Human and Experimental Toxicology **14**(11): 857-864.

Glynn, P. (1999). "Neuropathy target esterase." Biochem. J. **344**(3): 625-631.

Gutierrez, D. (2009). "Airplane Cabin Air Filled with Toxic Chemicals." Retrieved June 2009, 2009, from http://www.naturalnews.com/025990.html.

Habboush, A. E., et al. (1995). "Extraction-gas chromatographic method for the determination of organophosphorus compounds as lubricating oil additives." <u>Journal of Chromatography A</u> **696**(2): 257.

Haslam, J. and Squirrell, D. C. M. (1952). "The determination of o-tolyl ester in tritolyl phosphate." **77**: 71-74.

Hitchman, M. L. and Ramanathan, S. (1988). "Evaluation of iridium oxide electrodes formed by potential cycling as pH probes." <u>The Analyst</u> **113**: 35-39.

http://www.epa.gov/pesticides/op/primer.htm. "Organophosphate Pesticide Tolerance Reassessment and Reregistration." <u>Pesticides: Organophosphates</u> Retrieved 7 February 2006, 2006, from http://www.epa.gov/pesticides/op/.

Hunt, E. H. and Space, D. R. "The Airplane Cabin Environment: Issues Pertaining to Flight Attendant Comfort." 2009, from http://www.boeing.com/commercial/cabinair/ventilation.pdf.

Johnson, M. K. (1970). "Organophosphorus and other inhibitors of brain `neurotoxic esterase' and the development of delayed neurotoxicity in hens." <u>Biochem. J.</u> **120**(3): 523-531.

Johnson, M. K. (1975). "Organophosphorus esters causing delayed neurotoxic effects: mechanism of action and structure activity studies." Archives of Toxicology **34**(4): 259-288.

Joseph, R. S., et al. (2003). "Sensors, Chemical Sensors, Electrochemical Sensors, and ECS." Journal of The Electrochemical Society **150**(2): S11-S16.

Katsube, T., et al. (1981). "pH-sensitive sputtered iridium oxide films." Sensors and Actuators **2**: 399.

Kenmotsu, K., et al. (1983). "An environmental survey of chemicals. XXII. GC/MS spectrometric determination of organophosphoric acid triesters in sediment." Okayama-ken Kankyo Hoken Senta Nempo **7**: 143-149.

Kittiwake. (2009). "Kittiwake Monitoring Innovations:Oil test solutions." 2009, from http://www.kittiwake.com/docs/MA-K27467-KW_Oil_Test_Solutions_Flyer.pdf.

Lai, K., et al. (1994). "Bimetallic binding motifs in organophosphorus hydrolase are important for catalysis and structural organization." Journal of Biological Chemistry **269**(24): 16579-16584.

Lauks, I., et al. (1983). "Electrically free-standing IrOitx thin film electrodes for high temprature, corrosive environment pH sensing." Sensors and Actuators **4**: 375.

Leland, C. C., Jr. and Champ, L. (1962). "Electrode systems for continuous monitoring in cardiovascular surgery." Annals of the New York Academy of Sciences **102**(Automated and Semi-Automated Systems in Clinical Chemistry): 29-45.

Lewis, V. E., et al. (1988). "Mechansism and steriochemical course at phosphorus of the reaction catalyzed by a baterial phosphotriesterase." Biochemistry **27**: 1591-1597.

Marzouk, S. A. M. (2003). "Improved Electrodeposited Iridium Oxide pH Sensor Fabricated on Etched Titanium Substrates." Analytical Chemistry **75**(6): 1258-1266.

Murawski, J. (2003). Association of flight attendants, AFL-CIO - Aircraft air quality: What's wrong with it and what needs to be done. Association, of, Flight and Attendents. Washington D. C., The Aviation Subcommittee of The Transportation & Infrastructure Committee U.S. House of Representatives**:** 1-40.

Netten, V. and Leung, V. (2000). "Comparison of the constituents of two jet engine lubricating oils and their volatile pyrolytic degradation products." Applied Occupational and Environmental Hygiene **15**(3): 277-283.

Olthuis, W., et al. (1990). "pH sensor properties of electrochemically grown iridium oxide." <u>Sensors and Actuators B: Chemical</u> **2**(4): 247.

Pásztor, K., et al. (1993). "Iridium oxide-based microelectrochemical transistors for pH sensing." <u>Sensors and Actuators B: Chemical</u> **12**(3): 225.

Perley, G. A. (1949). "Glasses for Measurement of pH." <u>Analytical Chemistry</u> **21**(3): 394-401.

Qiang, Z., et al. (2002). "Electrochemical Sensors Based on Carbon Nanotubes." <u>Electroanalysis</u> **14**(23): 1609-1613.

Quintana, J. B., et al. (2008). "Organophosphorus flame retardants and plasticizers in water and air II. Analytical methodology." <u>TrAC Trends in Analytical Chemistry</u> **27**(10): 904.

Ramanathan, M. and Simonian, A. L. (2007). "Array biosensor based on enzyme kinetics monitoring by fluorescence spectroscopy: Application for neurotoxins detection." <u>Biosensors and Bioelectronics</u> **22**(12): 3001-3007.

Ramsey, J. D., et al. (1980). "Gas--liquid chromatographic retention indices of 296 non-drug substances on SE-30 or OV-1 likely to be encountered in toxicological analyses." Journal of Chromatography **184**(2): 185-206.

Reemtsma, T., et al. (2008). "Organophosphorus flame retardants and plasticizers in water and air I. Occurrence and fate." TrAC Trends in Analytical Chemistry **27**(9): 727.

Schleeter, N. and McCalmont, M. (2005). "The oil sludge problem." 2009, from http://www.schleeter.com/images/BMW%20oil%20sludge.JPG.

Senannayake, N. and Karalliedde, L. (1987). "Neurotoxic effects of organophosphate insecticides: an intermediate syndrome." New England journal of Medicine **316**: 716-763.

Sheng, Y., et al. (2001). "A pH Electrode Based on Melt-Oxidized Iridium Oxide." Journal of The Electrochemical Society **148**(4): H29-H36.

Shervedani, R. K., et al. (2007). "Electrochemical Characterization and Application of Ni RuO2 as a pH Sensor for Determination of Petroleum Oil Acid Number." Journal of Iranian chemical society **4**(2): 221-228.

Shimizu, Y. and Yamashita, N. (2000). "Solid electrolyte CO2 sensor using NASICON and perovskite-type oxide electrode." Sensors and Actuators B: Chemical **64**(1-3): 102.

Simonian, A. L., et al. (2001). "Discriminative detection of neurotoxins in multi-component samples." Analytica Chimica Acta **444**(2): 179.

Simonian, A. L., et al. (1997). "A new approach for discriminative detection of organophosphate neurotoxins in the presence of other cholinesterase inhibitors." Analytical Letters **30**(4): 2453–2468.

Spengler, J. and Wilson, D. (2003). "Air quality in aircraft." Proceedings of the Institution of Mechanical Engineers, Part E: Journal of Process Mechanical Engineering **217**(4): 323.

Valentini, F., et al. (2007). "The electrochemical detection of ammonia in drinking water based on multi-walled carbon nanotube/copper nanoparticle composite paste electrodes." Sensors and Actuators B: Chemical **128**(1): 326.

Viveros, L., et al. "A fluorescence-based biosensor for the detection of organophosphate pesticides and chemical warfare agents." Sensors and Actuators B: Chemical **In Press, Corrected Proof**.

Viveros, L., et al. (2006). "A fluorescence-based biosensor for the detection of organophosphate pesticides and chemical warfare agents." Sensors and Actuators B: Chemical **115**(1): 150-157.

Wang, M., et al. (2002). "A long-term stable iridium oxide pH electrode." Sensors and Actuators B: Chemical **81**(2-3): 313.

Wang, S. S. (2001). "Road tests of oil condition sensor and sensing technique." Sensors and Actuators B: Chemical **73**(2-3): 106.

Wang, S. S. (2002). "Engine oil condition sensor: method for establishing correlation with total acid number." Sensors and Actuators B: Chemical **86**(2-3): 122.

Winder, C. and Balouet, J.-C. (2002). "The Toxicity of Commercial Jet Oils." Environmental Research **89**(2): 146.

Yamanaka, K. (1989). "Anodically electrodeposited iridium oxide films (AEIROF) from alkaline solutions for electrochromic display devices." Japanese journal of applied physics **28**: 632-637.

Zachariasen, W. H. (1932). "The atomic arrangement in glass." Journal of the American Chemical Society **54**(10): 3841-3851.